PHYSICAL REVIEW D VOLUME 32, NUMBER 9 1 NOVEMBER 1985

Variational quantum-field-theoretical approach to the chiral bag

J. N. Urbano* and K. Goeke†

Institut für Kernphysik, Kernforschungsanlage Jülich, D-5170 Jülich, West Germany

(Received 12 October 1984)

A variational quantum-field-theoretical approach to the chiral bag is presented in which the pion field is described by a quantum-mechanical coherent state coupled to the bag by the interaction Hamiltonian of the linearized cloudy-bag model. States with good spin and isospin quantum numbers are projected from variationally stable solutions. Techniques are explained in detail. The nucleon is stabilized against collapse by incorporating the finite extension of the pions in the field. The dependence of nucleon masses, bag radii, average pion numbers, and self-energies on the various parameters is investigated. The free parameters of the system are fixed by requiring the variational solutions to have the proper nucleon energy and the proper pion-nucleon vertex. Bag radii of ~ 0.5 fm are obtained for certain parameter sets if Δ degrees of freedom are considered in the bag's wave function. For this and other features quantum fluctuations are shown to be important.

I. INTRODUCTION

There is at present a considerable interest in the study of a variety of phenomenological models for baryons in which quarks are coupled to meson fields.[1-13] This interest is motivated by the belief that such models may bridge the gap between the fundamental theory of strong interactions, i.e., quantum chromodynamics, and the best-known manifestation of these forces, i.e., the realm of nuclear physics. There is hope that from the study of these phenomenological models one can acquire a better understanding of hadron properties at low and intermediate energies.

One of the most successful classes of chiral-invariant models consists of chiral bag theories, in which the quarks are, from the start, confined to a certain domain in space.[8-12] Other examples are given, e.g., by the σ models in which the binding of the valence quarks is to be obtained as a result of the theory.[1-4,6] In these and other chiral-invariant approaches extensive use is made of classical or mean-field approximations for the meson fields which usually violate spin and isospin symmetries. Only in perturbational approaches of low order fully symmetry-conserving treatments seem to be possible at present. This is very unsatisfactory if one is interested, for instance, in exploring the possibility of having solutions for the nucleon with bag radii of 0.5 fm or smaller. For these studies there is a need for nonperturbative and symmetry-conserving theories, which are thus able to treat strong meson fields. The purpose of the present paper is to present such a theory. For this purpose the quark structure of the mesons is suppressed in favor of treating them as a separate field described by a coherent state. We make use of well-established projection techniques in order to extract quantum states with good angular momentum and isospin quantum numbers. This quantum-mechanical treatment involving the semiclassical coherent states is motivated, on the one hand, by some success of classical descriptions[3-6] and, on the other hand, by the obvious need for the inclusion of quantum fluctuations.[2,3] It has the interesting feature that the classical fields can be extracted as expectation values of the proper quantum-field operators between a variational solution of a suitable quantum-field-theoretical Hamiltonian for the whole system. This is in contrast to many recent approaches where the mesons are described from the start by c-number fields[3,4] for which one does not know how to quantize properly.

The present approach is formulated by investigating as a practical example some nucleon properties. We work in the conceptual frame of chiral-bag models[7-12] and adopt the quantized Hamiltonian of the linearized cloudy-bag model.[12] The formalism stabilizes the bag against the collapse[14] caused by the increasing pressure of the pion field with decreasing bag radius. This is done by assuming pions to have a finite size, in a way similar to the one recently suggested by Kam and Pirner.[15] We evaluate the effect of quantum fluctuations of the pion field by projections on good angular momentum and isospin quantum numbers. It turns out that they are indeed quite important and that they smooth the dependence of the nucleon energy on the bag radius. Solutions with small bag radii seem to be possible for certain choices of parameters and after the inclusion of Δ degrees of freedom. These solutions are self-consistent since they are obtained with a proper vertex renormalization.

The paper is constructed as follows. In Sec. II the Hamiltonian for the system consisting of a bag and a pion field is derived and the finite size of the pions is incorporated in the interaction Hamiltonian. The variational principle with a suitable trial wave function is presented in Sec. III and the intrinsic self-energy of the nucleon bag is evaluated. The angular momentum and isospin projections are performed in Sec. IV and the vertex renormalization in Sec. V. The possible existence of "little-bag" solutions is discussed in Sec. VI. Parts of this section have already been published in a Letter.[16] A summary and some conclusions are given in Sec. VII. There are several appendices to present the technical details of the approach.

II. THE HAMILTONIAN

A. The formalism with elementary pions

The Hamiltonian of the bag interacting with the elementary pion field is written

$$\hat{H}=\hat{H}_{\rm MIT}+\hat{H}_\pi+\hat{H}_{\rm coupl}\ , \tag{2.1}$$

where $\hat{H}_{\rm MIT}$ is the Hamiltonian of the MIT bag model,[17]

$$\hat{H}_{\rm MIT}=\int d^3\mathbf{r}\left[\frac{i}{2}\sum_a \hat{q}_a^\dagger(\mathbf{r})\overleftrightarrow{\partial}_0\hat{q}_a(\mathbf{r})+B\right]\theta_v\ , \tag{2.2}$$

with $\theta_v=1$ inside and $\theta_v=0$ outside the bag. The $\hat{H}_\pi$ denotes the energy operator of the free pion field,

$$\hat{H}_\pi=\sum_j\int d^3\mathbf{k}\,\omega(\mathbf{k})a_j^\dagger(\mathbf{k})a_j(\mathbf{k})\ , \tag{2.3}$$

and the quark-pion coupling term reads, in the linearized version of the cloudy-bag model,[12]

$$\hat{H}_{\rm coupl}=\frac{i}{2f}\int d^3\mathbf{r}\sum_a \hat{\bar{q}}_a(\mathbf{r})\gamma_5\vec{\tau}_a\cdot\hat{\vec{\phi}}(\mathbf{r})\hat{q}_a(\mathbf{r})\Delta_s\ . \tag{2.4}$$

Here the pion field is given by its usual expansion

$$\hat{\phi}_j(\mathbf{r})=(2\pi)^{-3/2}\int d^3\mathbf{k}[2\omega(\mathbf{k})]^{-1/2}[a_j(\mathbf{k})e^{i\mathbf{k}\cdot\mathbf{r}}+a_j^\dagger(\mathbf{k})e^{-i\mathbf{k}\cdot\mathbf{r}}]$$

with

$$\omega(\mathbf{k})=(\mathbf{k}^2+m_\pi{}^2)^{1/2}\ . \tag{2.5}$$

In Eq. (2.4) the sum extends over the three quark colors, and Δ_s is a surface δ function at the bag's surface. The $a_j^\dagger(\mathbf{k})$ create a pion with momentum $\mathbf{k}$ and Cartesian isospin component j. In the representation of the complete set of colorless baryonic bag states[12] $|B_n\rangle$ the $\hat{H}_{\rm MIT}$ can be written as

$$\hat{H}_{\rm MIT}=\sum_n E_{B_n}|B_n\rangle\langle B_n| \tag{2.6}$$

with E_{B_n} being the energy of the states $|B_n\rangle$. The interaction $\hat{H}_{\rm coupl}$ has nondiagonal terms

$$\hat{H}_{\rm coupl}=\frac{i}{2f}\sum_{n,m}|B_n\rangle\langle B_n|\times\int d^3\mathbf{r}\sum_a\hat{\bar{q}}_a(\mathbf{r})\gamma_5\vec{\tau}_a\hat{q}_a(\mathbf{r})\cdot\hat{\vec{\phi}}(\mathbf{r})\times\Delta_s|B_m\rangle\langle B_m|\ . \tag{2.7}$$

In the present paper we restrict the $|B_n\rangle$ to the nucleon ground state $|N\rangle$ and the Δ isobar $|\Delta\rangle$. This choice takes into account to some extent the spin-isospin-flip degrees of freedom and has in addition the technical advantage that the radial quark wave functions all correspond to the lowest s state. In such a case one obtains (see Appendix A)

$$\hat{H}_{\rm coupl}=i\int d^3k\, f_R(k)\sum_j[\hat{X}_j(\mathbf{k})a_j(\mathbf{k})-\hat{X}_j^\dagger(\mathbf{k})a_j^\dagger(\mathbf{k})] \tag{2.8}$$

with

$$f_R(k)=\rho_R(k)[2\omega(k)(2\pi)^3]^{-1/2}\ , \tag{2.9}$$

where $\rho_R(k)$ plays the role of the Fourier transform of the density of the pion source. For a bag with radius R one has

$$\rho_R(k)=3\frac{j_1(kR)}{kR} \tag{2.10}$$

which will in the following always be approximated[13] by

$$\rho_R(k)=e^{-0.106R^2k^2}\ . \tag{2.11}$$

The Hermitian operators $X_j(\mathbf{k})$ depend on the actual choice of $|N\rangle$ and $|\Delta\rangle$. For a nucleon with spin and isospin components $s,t=\pm\frac{1}{2}$ and a Δ with corresponding components $S,T=\pm\frac{1}{2},\pm\frac{3}{2}$ one obtains

$$\hat{X}_j(\mathbf{k})=\hat{X}_j^{\pi NN}(\mathbf{k})+\hat{X}_j^{\pi N\Delta}(\mathbf{k})+\hat{X}_j^{\pi\Delta N}(\mathbf{k})+\hat{X}_j^{\pi\Delta\Delta}(\mathbf{k})\ , \tag{2.12}$$

with

$$\hat{X}_j^{\pi NN}(\mathbf{k})=g_{\pi NN}\sum_{st}^{1/2}\sum_{s',t'}^{1/2}(\sigma\cdot\mathbf{k})_{s,s'}(\tau_j)_{t,t'}\hat{\nu}_{st}^\dagger\hat{\nu}_{s't'}\ , \tag{2.13a}$$

$$\hat{X}_j^{\pi N\Delta}(\mathbf{k})=g_{\pi N\Delta}\sum_{st}^{1/2}\sum_{ST}^{3/2}(\mathbf{S}\cdot\mathbf{k})_{S,s}(T_j)_{T,t}\hat{\delta}_{ST}^\dagger\hat{\nu}_{st}\ , \tag{2.13b}$$

$$\hat{X}_j^{\pi\Delta N}(\mathbf{k})=g_{\pi\Delta N}\sum_{ST}^{3/2}\sum_{st}^{1/2}(S^\dagger\cdot\mathbf{k})_{s,S}(T_j^\dagger)_{t,T}\hat{\nu}_{st}^\dagger\delta_{ST}\ , \tag{2.13c}$$

$$\hat{X}_j^{\pi\Delta\Delta}(\mathbf{k})=g_{\pi\Delta\Delta}\sum_{ST}^{3/2}\sum_{S'T}^{3/2}(\Sigma\cdot\mathbf{k})_{S,S'}(\theta_j)_{T,T'}\delta_{ST}^\dagger\hat{\delta}_{S'T'}\ . \tag{2.13d}$$

Here the coupling constants are related through

$$g_{\pi\Delta\Delta}=\tfrac{4}{5}g_{\pi NN}\ , \tag{2.14a}$$

$$g_{\pi N\Delta}=g_{\pi\Delta N}=(\tfrac{72}{25})^{1/2}g_{\pi NN}\ , \tag{2.14b}$$

$$g_{\pi NN}=\frac{1}{2f}\frac{\Omega}{\Omega-1}\frac{5}{9}\ , \tag{2.14c}$$

with $\Omega=2.04$. If there were no pions the $g_{\pi NN}$ should be equal to $g_{\pi NN}=(4\pi)^{1/2}f_{\pi NN}/m_\pi=7.25$ GeV^{-1} with $f_{\pi NN}{}^2=0.082$. In the present theory, however, the $g_{\pi NN}$ is not known *a priori*. It has to be determined by a proper renormalization as described in Sec. V. The matrices σ, S, etc., are spin matrices and are explicitly given in Appendix A. The operators $\hat{\nu}_{st}^\dagger$ ($\hat{\nu}_{st}$) and $\hat{\delta}_{ST}^\dagger$ ($\hat{\delta}_{ST}$) create (annihilate) nucleons and Δ's with spin and isospin components s,t and S,T, respectively. With Eqs. (2.3), (2.6), and (2.8) the Hamiltonian of the system is specified. In the following we assume

$$E_N(R)=E_\Delta(R)=\frac{3\Omega}{R}+\frac{4\pi}{3}BR^3-\frac{Z}{R}\ , \tag{2.15}$$

with B being the volume energy parameters. The term Z/R accounts for the corrections to the quark kinetic energy from spurious center-of-mass contributions and contributions from the quantization of the gluon field in a cavity. As yet the coefficient Z cannot be reliably determined from more fundamental considerations. The total

Hamiltonian depends on the bag radius R because of this choice of E_N and of $H_{\rm coupl}$. In the MIT model the E_Δ is different from E_N due to the different residual quark-gluon coupling, which is supposed to account for the whole mass difference. Since we are presently interested in the mass difference coming from the pion cloud we assume $E_\Delta = E_N$ in order to avoid another free parameter. This does not affect, however, our main conclusions concerning the nucleon ground state.

B. Pions with finite size

As is well known[14]—and this will come out quite clearly from the present variational formalism—the total energy of the bag coupled at the surface to the elementary pion cloud is not stable. With decreasing bag radius R, after a certain point the strength of the pion field increases without limit, leading eventually to a collapse for $R \to 0$. Recently several mechanisms have been suggested to prevent this.[15,18–20] In the present approach we follow the one proposed by Kam and Pirner[15] which consists in modifying the interaction Lagrangian density by taking into account the finite size of the pions. For a real pion[21] the extension η_π of the $q\bar{q}$ components, relevant for the coupling, is related to the pion decay constant f_π by[22] $\eta_\pi = (4\pi f_\pi)^{-1} = 0.17$ fm. This relation, however, does not directly apply to the virtual pions constituting the pion cloud. Therefore, to be on the safe side, we consider a range of η_π values

$$0.12 \le \eta_\pi \le 0.4 \text{ fm} . \tag{2.16}$$

The results are to a large extent independent of the actual choice of η_π within this range. The Hamiltonian density which describes the pion-quark interaction—see Eq. (2.4)—is then modified to the nonlocal form

$$\mathscr{H}^{\rm mod}_{\rm coupl}(\mathbf{r}) = \frac{1}{2f} \sum_a \int d^3\eta\, \hat{\bar{q}}_a(\mathbf{r}+\boldsymbol{\eta})\gamma_5 \vec{\tau}_a \hat{q}_a(\mathbf{r}-\boldsymbol{\eta}) \cdot \hat{\vec{\phi}} \times \delta(r-R) P(\boldsymbol{\eta}) , \tag{2.17}$$

with $P(\boldsymbol{\eta})$ being the probability of finding a quark and antiquark at a relative distance 2η in the extended pion. We take it as a Gaussian, following Brodsky and Lepage,[22]

$$P(\boldsymbol{\eta}) = (\pi\eta_\pi^{\,2})^{-3/2} \exp\left[-\left[\frac{\eta}{\eta_\pi}\right]^2\right] . \tag{2.18}$$

For the technical evaluation of the modified interaction Lagrangian it is convenient to replace the Bessel j_0 and j_1 functions in the quark wave function

$$q_a(\mathbf{r}) = \frac{N}{\sqrt{4\pi}} \begin{bmatrix} j_0\left[\dfrac{r\Omega}{R}\right] \\ ij_1\left[\dfrac{r\Omega}{R}\right]\boldsymbol{\sigma}\cdot\hat{\mathbf{r}} \end{bmatrix} u_a \tag{2.19}$$

by Gaussians. For $\Omega = 2.04$ these expressions can be found in Ref. 15 and are listed here for completeness,

$$j_0\left[\frac{\Omega r}{R}\right] \cong \exp\left[-C_3\left[\frac{r}{R}\right]^2\right]\left[1-C_1\left[\frac{r}{R}\right]^2\right] , \tag{2.20a}$$

$$j_1\left[\frac{\Omega r}{R}\right] \cong \exp\left[-C_3\left[\frac{r}{R}\right]^2\right] C_2\left[\frac{r}{R}\right] \tag{2.20b}$$

with $C_1 = 0.21$, $C_2 = 0.80$, and $C_3 = 0.59$. Inserting this into Eq. (2.17) one obtains (see Appendix B for details) the modified interaction Hamiltonian density

$$\mathscr{H}^{\rm mod}_{\rm coupl}(\mathbf{r}) = M(\eta_\pi, R, r)\mathscr{H}_{\rm coupl}(\mathbf{r}) \tag{2.21}$$

with

$$M(\eta_\pi,R,r) = \left[1+2C_3\left[\frac{\eta_\pi}{R}\right]^2\right]^{-3/2} \times \left\{1 - \frac{C_1\left[\dfrac{\eta_\pi}{R}\right]^2}{2\left[1+2C_3\left[\dfrac{\eta_\pi}{R}\right]^2\right]\left[1-C_1\left[\dfrac{r}{R}\right]^2\right]}\right\} . \tag{2.22}$$

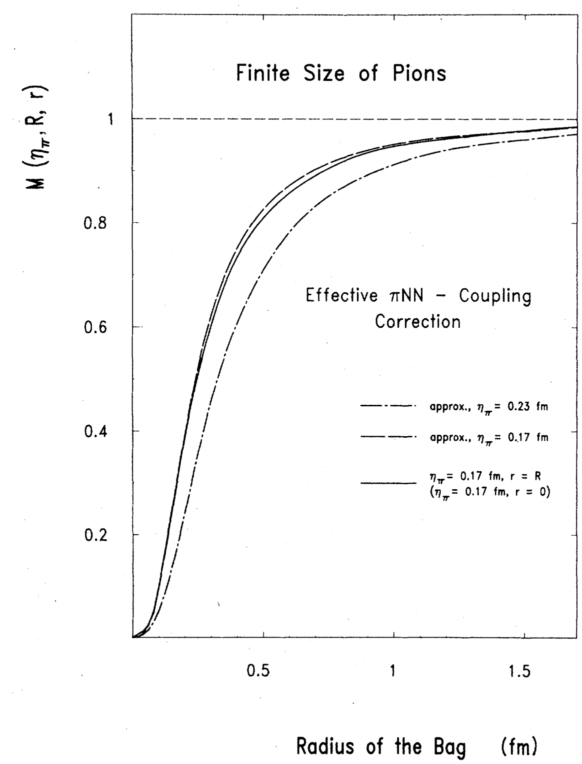

FIG. 1. The correction factor $M(\eta_\pi,R,r)$ of the pion-nucleon coupling constant due to the finite size of the pion. Plotted are the exact expression of Eq. (2.22) and the approximations to it in (2.23). Thus the curves correspond to $g_{\rm eff}(R)/g_{\pi NN}$.

For $\eta_\pi \to 0$ the $M(\eta_\pi,R,r)\to 1$ and the elementary pion-field approximation is recovered. For finite η_π the $M(\eta_\pi,R,r)$ is r dependent. This dependence, however, is so weak that on Fig. 1 the difference between the curves with $r=0$ and $r=R$ is not visible. In addition, for computational reasons we simplify $M(\eta_\pi,R,r)$ by ignoring the second term in Eq. (2.22). This approximation is a rather good one as one can see at Fig. 1 as well.

Hence the effect of the finite extension of the pion amounts altogether to a renormalized and R-dependent coupling constant $g_{\mathrm{eff}}(R)$ to replace the g in the coupling Hamiltonian (2.8) and (2.13),

$$g_{\pi NN}\to g_{\mathrm{eff}}(R)=g_{\pi NN}\left[1+2C_3\left[\frac{\eta_\pi}{R}\right]^2\right]^{-3/2} . \tag{2.23}$$

As one sees immediately, this coupling constant goes to zero for $R\to 0$, which prevents the collapse of the nucleon.

III. THE VARIATIONAL PRINCIPLE

A. The trial wave function

The nucleon model consists of a bag of quarks and a pion field. The bag state $|BN\rangle$ is assumed to have spin and isospin z components both equal to $\frac{1}{2}$. Since it is coupled to the pion field, which also carries angular momentum and isospin, it is not necessary for $|BN\rangle$ to carry the quantum numbers of the nucleon itself, i.e., spin and isospin $\frac{1}{2}$. We assume the $|BN\rangle$ to be a mixture between states with total nucleon and Δ quantum numbers to be consistent with the vertices used in the interaction Hamiltonian:

$$|BN(\alpha)\rangle=\cos\alpha\,|N_{1/2}^{+}\rangle+\sin\alpha\,|\Delta_{1/2}^{+}\rangle . \tag{3.1}$$

Here $|N_{1/2}^{+}\rangle$ and $|\Delta_{1/2}^{+}\rangle$ correspond to a nucleon and Δ with one elementary charge and spin component $\frac{1}{2}$. They are normalized to unity. The pion field is described as a coherent state[23]

$$|\pi(\xi)\rangle=N^{-1/2}\exp\left[\sum_j\int d^3\mathbf{k}\,\xi_j(\mathbf{k})a_j^{\dagger}(\mathbf{k})\right]|0\rangle , \tag{3.2a}$$

with

$$N=\exp\left[\sum_j\int d^3k\,\xi_j^{*}(\mathbf{k})\xi_j(\mathbf{k})\right] \tag{3.2b}$$

and $\xi(\mathbf{k})$ being the pion field amplitude (expansion coefficient) to be determined variationally. The coherent state has the important property

$$a_j(\mathbf{k})\,|\pi(\xi)\rangle=\xi_j(\mathbf{k})\,|\pi(\xi)\rangle . \tag{3.3}$$

The product state

$$|\xi,\alpha,R\rangle=|\pi(\xi)\rangle\,|BN(\alpha)\rangle \tag{3.4}$$

does not possess the spin and isospin quantum numbers of a nucleon or of its isobars. These, however, can be extracted by means of the Peierls-Yoccoz projection techniques[16,24]

$$|\Psi_{JJ_z,TT_z}(\xi,\alpha,R)\rangle=\frac{P_{JJ_z}P_{TT_z}\,|\xi,\alpha,R\rangle}{\left[\sum_{K,L}\langle\xi,\alpha,R\,|P_{JK}P_{TL}|\,\xi,\alpha,R\rangle\right]^{1/2}} , \tag{3.5}$$

whose details will be described in Sec. III B. The appropriate variational procedure would be now to vary, with respect to ξ, R, and α, the energy of the physical baryon

$$E_{JT}(\xi,\alpha,R)=\frac{\langle\xi,\alpha,R\,|\hat{H}P_JP_T|\,\xi,\alpha,R\rangle}{\langle\xi,\alpha,R\,|P_JP_T|\,\xi,\alpha,R\rangle} \tag{3.6}$$

into its minimum. The variable R at the energy indicates that it depends on the radius R of the bag chosen. Actually, because of technical reasons, we do perform such a projection before the variation only with respect to R and α, but will do a projection after the variation with respect to ξ.

B. The intrinsic energy

The intrinsic energy $E_{\mathrm{intr}}(\xi,\alpha,R)$ is given by

$$E_{\mathrm{intr}}(\xi,\alpha,R)=\frac{\langle\xi,\alpha,R\,|\hat{H}|\,\xi,\alpha,R\rangle}{\langle\xi,\alpha,R\,|\,\xi,\alpha,R\rangle} . \tag{3.7}$$

Since in this expression the fluctuations of the fields due to spin and isospin are neglected the evaluation of the intrinsic energy corresponds to calculating the energy of the system in a mean-field approximation. This is a point worth noticing. Inserting Eq. (2.1) into Eq. (3.7) one obtains

$$E_{\mathrm{intr}}(\xi,\alpha,R)=E_{\mathrm{BN}}^{\mathrm{intr}}(\xi,\alpha,R)+E_{\pi}^{\mathrm{intr}}(\xi,\alpha,R)+E_{\mathrm{coupl}}^{\mathrm{intr}}(\xi,\alpha,R) . \tag{3.8}$$

Inserting Eqs. (3.4), (3.1), and (2.6) into Eq. (3.8) one obtains immediately

$$E_{BN}^{\mathrm{intr}}(\xi,\alpha,R)=E_N\cos^2\alpha+E_\Delta\sin^2\alpha . \tag{3.9}$$

Inserting now Eqs. (2.3) and (3.2) into Eq. (3.8) and using Eq. (3.3) yields

$$E_{\pi}^{\mathrm{intr}}(\xi,\alpha,R)=\sum_j\int d^3k\,\omega(k)\xi_j^{*}(\mathbf{k})\xi_j(\mathbf{k}) . \tag{3.10}$$

The interaction energy is similarly evaluated by using Eqs. (2.8) and (3.2)—(3.4). It yields immediately

$$E_{\mathrm{coupl}}^{\mathrm{intr}}(\xi,\alpha,R)=i\int d^3k\,f_R(k)\times\sum_j[\langle BN(\alpha)\,|\hat{X}_j(\mathbf{k})|\,BN(\alpha)\rangle\xi_j(\mathbf{k})-\langle BN(\alpha)\,|\hat{X}_j^{\dagger}(\mathbf{k})|\,BN(\alpha)\rangle\xi_j^{*}(\mathbf{k})] \tag{3.11}$$

with $f_R(k)$ given by Eq. (2.9). The intrinsic state $|\xi,\alpha,R\rangle$ is now obtained by Ritz's variation of $E_{\mathrm{intr}}(\xi,\alpha,R)$ with respect to ξ, α, and R. The variation of the pion field corresponds to

$$\frac{\delta}{\delta \xi_j^*(\mathbf{k})} E_{\text{intr}}(\xi,\alpha,R)=0 \tag{3.12}$$

or equivalently

$$\omega(k)\xi_j(\mathbf{k})-if_R(k)\langle BN(\alpha)\,|\,\hat{X}_j^\dagger(\mathbf{k})\,|\,BN(\alpha)\rangle=0\ . \tag{3.13}$$

Since $\hat{X}_j(\mathbf{k})$ is Hermitian, one hence obtains for the variational solution, indicated by an overbar,

$$\bar{\xi}_j(\mathbf{k})=i\frac{f_R(k)}{\omega(k)}\langle BN(\alpha)\,|\,\hat{X}_j(\mathbf{k})\,|\,BN(\alpha)\rangle\ . \tag{3.14}$$

The $\bar{\xi}_j(k)$ depends on R, although it is not indicated. Inserting this into Eq. (3.8) we have

$$E_{\text{coupl}}^{\text{intr}}(\alpha,R)=-2E_\pi^{\text{intr}}(\alpha,R) \tag{3.15}$$

with the total intrinsic energy of the system

$$E_{\text{intr}}(\alpha,R)=E_N\cos^2\alpha+E_\Delta\sin^2\alpha+E_{\text{intr}}^{\text{SE}}(\alpha,R) \tag{3.16}$$

and the intrinsic self-energy given by

$$E_{\text{intr}}^{\text{SE}}(\alpha,R)=-\int d^3k\frac{f_R{}^2(k)}{\omega(k)}\sum_j |\langle BN(\alpha)\,|\,\hat{X}_j(\mathbf{k})\,|\,BN(\alpha)\rangle|^2\ . \tag{3.17}$$

The explicit evaluation of the matrix element in Eq. (3.14) yields, with Eq. (2.12) and the matrices of Appendix A,

$$\bar{\xi}_j(\mathbf{k})=i\frac{f_R(k)}{\omega(k)}g_{\pi NN}G(\alpha)k_z\delta_{j3} \tag{3.18}$$

with

$$G(\alpha)=\cos^2\alpha+\frac{8\sqrt{2}}{5}\sin\alpha\cos\alpha+\tfrac{1}{5}\sin^2\alpha\ . \tag{3.19}$$

The function $G(\alpha)$ can be considered as a renormalization of the coupling constant $g_{\pi NN}$ due to the inclusion of the Δ degrees of freedom in the bare nucleon configuration. A graph of $G^2(\alpha)$ is given in Fig. 2. For the evaluation of $E_{\text{intr}}^{\text{SE}}(\alpha,R)$ it now remains to perform the integration over $\mathbf{k}$. This yields, using Eq. (B4) of Appendix B,

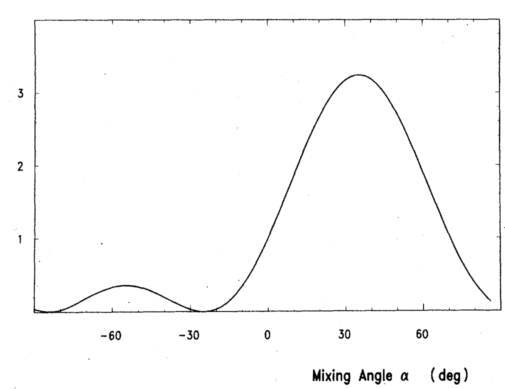

FIG. 2. The mixing function $G^2(\alpha)$ [cf. Eq. (3.19)] determining the admixture of Δ degrees of freedom to the nucleon ground state.

$$E_{\text{intr}}^{\text{SE}}(\alpha,R)=-E_{\text{intr}}^{\pi}(\alpha,R)=-\frac{g_{\pi NN}{}^2}{12\pi^2}G^2(\alpha)\int_0^\infty dk\frac{\rho_R{}^2(k)k^4}{k^2+m_\pi{}^2}\ . \tag{3.20}$$

This is the intrinsic self-energy of the bag which the wave function (3.1) acquires due to the coupling to the pion field.

Before we show some numerical results for the intrinsic nucleon energy we discuss the properties of the pion field, which arise from our variational procedure. The special structure of the amplitude (3.18) is due to our special choice of the bare nucleon configuration being aligned along the z direction in both spin and isospin spaces. It can equivalently be written as

$$\bar{\xi}_j(\mathbf{k})=i\frac{f_R(k)}{\omega(k)}g_{\pi NN}(\alpha)\langle N_{1/2}^+\,|\,\boldsymbol{\sigma}\cdot\mathbf{k}\tau_j\,|\,N_{1/2}^+\rangle\ , \tag{3.21}$$

where $g_{\pi NN}(\alpha)=g_{\pi NN}G(\alpha)$ is the renormalized coupling constant. In our formalism the classical pion field $\phi_j(\mathbf{r})$ is given by the expectation value of the quantized field operator $\hat{\phi}_j(\mathbf{r})$ of Eq. (2.5) between the coherent states (3.2):

$$\phi_j(\mathbf{r})=\langle\pi(\xi)\,|\,\phi_j(\mathbf{r})\,|\,\pi(\xi)\rangle\ . \tag{3.22}$$

This gives with Eqs. (3.3), (3.21), and (2.9)

$$\phi_j(\mathbf{r})=g_{\pi NN}(\alpha)\int\frac{\rho_R(k)}{[2\omega(k)]^{3/2}}\langle N_{1/2}^+\,|\,\boldsymbol{\sigma}\cdot\mathbf{k}\tau_j\,|\,N_{1/2}^+\rangle \times\frac{e^{i\mathbf{k}\cdot\mathbf{r}}-e^{-i\mathbf{k}\cdot\mathbf{r}}}{[2\omega(k)]^{1/2}}\frac{d^3k}{8\pi^3} \tag{3.23}$$

which can be simplified to

$$\phi_j(\mathbf{r})=ig_{\pi NN}(\alpha)\langle N_{1/2}^+\,|\,\boldsymbol{\sigma}\cdot\nabla\tau_j\,|\,N_{1/2}^+\rangle Y(\mathbf{r}) \tag{3.24}$$

with

$$Y(\mathbf{r})=\int d^3r'\rho_R(\mathbf{r}')\frac{e^{-m_\pi|\mathbf{r}-\mathbf{r}'|}}{4\pi|\mathbf{r}-\mathbf{r}'|}\ , \tag{3.25}$$

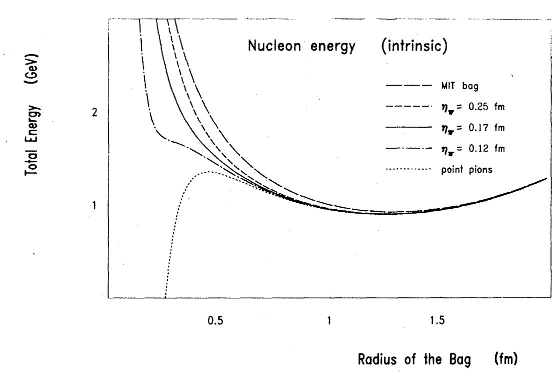

FIG. 3. The nucleon energy vs the bag radius R is plotted for the MIT bag model of Eq. (2.15) and for the intrinsic (nonprojected) variational solutions (assuming $\alpha=0$) using various pion radii η_π. The dotted curve, corresponding to point pions, shows the collapse as $R\rightarrow 0$. The calculations are done with $B^{1/4}=0.125$ GeV, $g_{\pi NN}=14$ GeV^{-1}, $Z=1.75$, and assuming $\alpha=0$.

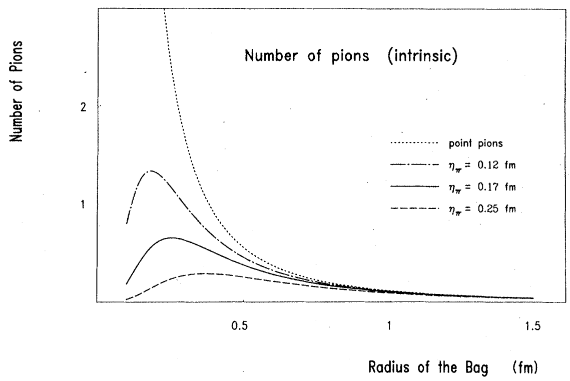

FIG. 4. The average number of pions in the pion cloud of the intrinsic (nonprojected) state as a function of the bag radius for various pion size parameters η_π. See caption to Fig. 3 for the parameter values.

where $\rho_R(\mathbf{r})$ is the Fourier transform of $\rho_R(\mathbf{k})$. This is the usual[25] expression for the classical Yukawa field produced by a source of density distribution $\rho_R(\mathbf{r})$.

For the evaluation of the intrinsic energy the integrations in Eq. (3.20) are performed numerically by means of Gauss-Hermite quadrature. Assuming a pure nucleon configuration of the bag, Fig. 3 shows some of our intrinsic energies for several pion radii in comparison to the MIT-bag energy. For pointlike pions there is a local minimum at $R \approx 1.2$ fm but the system collapses at small bag radii. This collapse is avoided if one takes into account the finite pion size by using $\eta_\pi \neq 0$.

The effect of the finite size of the pions can also be demonstrated by considering the average number of pions in the cloud. This is given by

$$N^\pi_{\text{intr}}(\alpha,R)=\frac{\langle \xi,\alpha,R \mid \hat{N} \mid \xi,\alpha,R \rangle}{\langle \xi,\alpha,R \mid \xi,\alpha,R \rangle} \ . \tag{3.26}$$

With

$$\hat{N}=\sum_{j=1}^{3} \int d^3k \, a_j^\dagger(\mathbf{k}) a_j(\mathbf{k}) \tag{3.27}$$

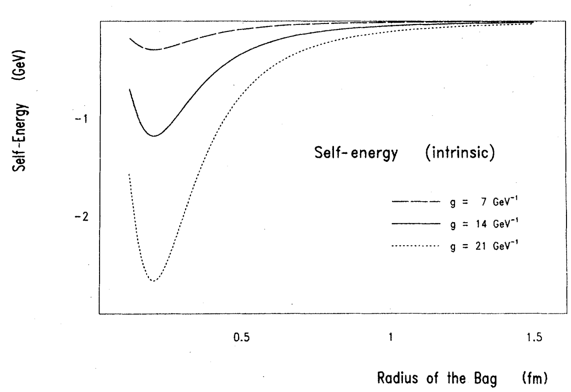

FIG. 5. The self-energy of the system, see Eqs. (3.16) and (3.17), for various values of the pion-bag coupling constant $g_{\pi NN}$. The calculations are done with $\eta_\pi = 0.17$ fm, $B^{1/4} = 0.125$ GeV, $Z = 1.75$, and assuming $\alpha = 0$.

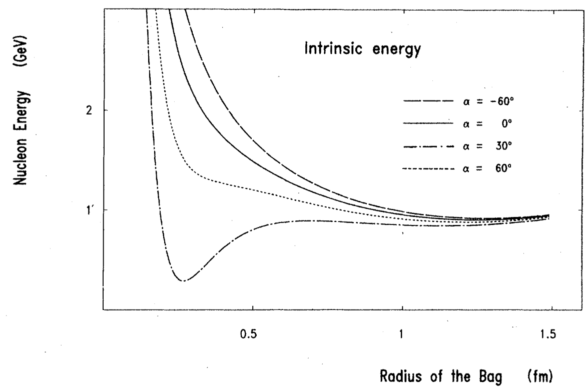

FIG. 6. The total intrinsic energy of bag plus pion cloud is plotted vs the bag radius R for various mixing angles α. The calculations are performed for $\eta_\pi = 0.17$ fm, $B^{1/4} = 0.125$ GeV, $Z = 1.75$, and $g_{\pi NN} = 14\ \text{GeV}^{-1}$.

this yields immediately

$$N^\pi_{\text{intr}}(\alpha)=\sum_{j=1}^{3} \int d^3k \, \bar{\xi}_j^*(\mathbf{k}) \bar{\xi}_j(\mathbf{k}) \tag{3.28}$$

or

$$N^\pi_{\text{intr}}(\alpha)=\frac{g_{\pi NN}{}^2}{12\pi^2} G^2(\alpha) \int dk \frac{\rho_R{}^2(k) k^4}{(k^2+m_\pi{}^2)^{3/2}} \ . \tag{3.29}$$

For $\alpha = 0$ the N_π^{intr} is plotted versus R in Fig. 4. In the case of point pions one realizes that N_π^{intr} diverges for $R \to 0$. However, for finite η_π the N_π^{intr} tends to zero in this limit. This feature is caused by the vanishing effective pion-nucleon coupling constant $g_{\text{eff}}(R)$ (see, e.g., Fig. 1).

Actually all results of those calculations depend on the bare pion-nucleon coupling constant $g_{\pi NN}$. Figure 5 shows that the dependence of the intrinsic self-energies on $g_{\pi NN}$ is highly nonlinear. Figure 6 displays the effect of the Δ admixture on the intrinsic energy: Apparently for small R this is very pronounced showing the largest effect for $\alpha = 30^\circ$ in accordance with the behavior of $G^2(\alpha)$ in Fig. 2.

IV. ANGULAR MOMENTUM AND ISOSPIN PROJECTIONS

The states $|\bar{\xi},\alpha,R\rangle$ of the bag plus pion field do not have angular momentum and isospin as good quantum numbers both because of the general form for the bag states and the pion cloud. Using the techniques of Peierls and Yoccoz one can extract[16,24] from these states the components with good spin and isospin quantum numbers, as indicated already in Eq. (3.5). For the present choice of $|BN(\alpha)\rangle$, having a good z component of J and a good 3 component of T, the total state has the properties

$$J_z \,|\bar{\xi},\alpha,R\rangle = s \,|\bar{\xi},\alpha,R\rangle, \quad s=\tfrac{1}{2} \ , \tag{4.1a}$$

$$T_3 \,|\bar{\xi},\alpha,R\rangle = t \,|\bar{\xi},\alpha,R\rangle, \quad t=\tfrac{1}{2} \ . \tag{4.1b}$$

Referring to Eq. (3.20) one sees this easily for the isospin, since the Cartesian third component corresponds to an uncharged pion. In the case of the angular momentum one has to remember that pions have no intrinsic spin, and to notice that the z component of the orbital angular momentum can be written in k-space as proportional to $k_x d/dk_y - k_y d/dk_x$. Therefore the pion cloud associated with the variational solution $\bar{\xi}$ of Eq. (3.20) carries no angular momentum along the z axis. Taking this into account the energy of the projected state (3.5) simplifies to

$$E_{JT}^{(R)}(\alpha)=\frac{\int_0^{\pi}\sin\beta\,d\beta\int_0^{\pi}\sin\tilde{\beta}\,d\tilde{\beta}\,d_{ss}^{J}(\beta)d_{tt}^{T}(\tilde{\beta})h(\alpha;\beta\tilde{\beta})}{\int_0^{\pi}\sin\beta\,d\beta\int_0^{\pi}\sin\tilde{\beta}\,d\tilde{\beta}\,d_{ss}^{J}(\beta)d_{tt}^{T}(\tilde{\beta})n(\alpha;\beta\tilde{\beta})}\ , \tag{4.2}$$

with the overlap kernels

$$h(\alpha;\beta,\tilde{\beta})=\langle \bar{\xi},\alpha,R\mid \hat{H}R_y(\beta)R_2(\tilde{\beta})\mid \bar{\xi},\alpha,R\rangle\ , \tag{4.3a}$$

$$n(\alpha;\beta,\tilde{\beta})=\langle \bar{\xi},\alpha,R\mid R_y(\beta)R_2(\tilde{\beta})\mid \bar{\xi},\alpha,R\rangle\ . \tag{4.3b}$$

A. Norm overlap

Since we perform a projection after the variation of ξ the pion field is assumed to be fixed by Eq. (3.20). The operators $R_y(\beta)$ and $R_2(\beta)$ are given by

$$R_y(\beta)=R_y^{\text{bag}}(\beta)R_y^{\pi}(\beta)=\exp[i\beta(J_y^{\text{bag}}+J_y^{\pi})]\ , \tag{4.4a}$$

$$R_2(\tilde{\beta})=R_2^{\text{bag}}(\tilde{\beta})R_2^{\pi}(\tilde{\beta})=\exp[i\tilde{\beta}(T_2^{\text{bag}}+T_2^{\pi})] \tag{4.4b}$$

and they act on the entire system, i.e., bag plus meson cloud. Their action on the state $\mid BN(\alpha)\rangle$ is easy to evaluate:

$$\begin{aligned}\mid BN(\alpha;\beta\tilde{\beta})\rangle &= B_y^{\text{bag}}(\beta)R_2^{\text{bag}}(\tilde{\beta})\mid BN(\alpha)\rangle\\ &=\cos\alpha\sum_{st}^{1/2} d_{s\,1/2}^{1/2}(\beta)d_{t\,1/2}^{1/2}(\tilde{\beta})\mid N_{st}\rangle\\ &\quad+\sin\alpha\sum_{ST}^{1/2} d_{S\,1/2}^{3/2}(\beta)d_{T\,1/2}^{3/2}(\tilde{\beta})\mid \Delta_{ST}\rangle\ .\end{aligned} \tag{4.5}$$

Since $R_y^{\pi}(\beta)R_2^{\pi}(\tilde{\beta})\mid 0\rangle=\mid 0\rangle$ the action of the rotational operator on the coherent state $\pi(\bar{\xi})\rangle$ can be written as

$$\begin{aligned}\mid \pi(\alpha;\beta\tilde{\beta})\rangle &= R_y^{\pi}(\beta)R_2^{\pi}(\tilde{\beta})\mid \pi(\bar{\xi})\rangle\\ &=N^{-1/2}\exp\left[\sum_j\int d^3k\,\bar{\xi}_j(\mathbf{k})R_y(\beta)\right.\\ &\qquad\left.\times R_2(\tilde{\beta})a_j^{\dagger}(\mathbf{k})\right]\mid 0\rangle\ .\end{aligned} \tag{4.6}$$

The rotation around the y axis yields then

$$\begin{aligned}&\sum_j\int d^3k\,\bar{\xi}_j(\mathbf{k})R_y(\beta)a_j^{\dagger}(\mathbf{k})\mid 0\rangle\\ &\qquad=\sum_j\int d^3k\,\bar{\xi}_j[R_y^{-1}(\beta)\mathbf{k}]a_j^{\dagger}(\mathbf{k})\mid 0\rangle\end{aligned} \tag{4.7}$$

since it amounts to a change of the integration coordinates from $\mathbf{k}$ to $R_y\mathbf{k}$. If one denotes with $[R_2(\tilde{\beta})]_{j'j}$ the rotational matrix in a Cartesian vector space, we obtain for the pion field finally

$$\begin{aligned}&R_y^{\pi}(\beta)R_2^{\pi}(\tilde{\beta})\mid \pi(\bar{\xi})\rangle\\ &\qquad=N^{-1/2}\exp\left[\sum_j\int d^3k\,\bar{\xi}_j(\mathbf{k};\beta,\tilde{\beta})a_j^{\dagger}(\mathbf{k})\right]\mid 0\rangle\ ,\end{aligned} \tag{4.8}$$

with

$$\bar{\xi}_j(\mathbf{k};\beta,\tilde{\beta})=\sum_{j'}[R_2(\tilde{\beta})]_{jj'}\bar{\xi}_{j'}[R_y^{-1}(\beta)\mathbf{k}]\ . \tag{4.9}$$

Using the expressions (3.18) and Eq. (C1) of Appendix C one obtains explicitly by first applying R_y^{-1} to $\mathbf{k}$ and then taking the z component

$$\begin{aligned}\bar{\xi}_j(\mathbf{k};\beta\tilde{\beta})&=ig_{\pi NN}\frac{f_R(k)}{\omega(k)}G(\alpha)(-k_x\sin\beta+k_z\cos\beta)\\ &\quad\times(-\delta_{j1}\sin\tilde{\beta}+\delta_{j3}\cos\tilde{\beta})(1-\delta_{j2})\ .\end{aligned} \tag{4.10}$$

With Eqs. (4.5) and (4.8)–(4.10) the rotated bag-plus-field state is now defined. It remains to evaluate the norm and Hamiltonian kernels. The norm overlap is very simple:

$$n(\alpha;\beta,\tilde{\beta})=n_{\pi}(\alpha;\beta\tilde{\beta})n_{BN}(\alpha;\beta\tilde{\beta}) \tag{4.11}$$

with

$$\begin{aligned}n_{BN}(\alpha;\beta\tilde{\beta})&=\cos^2\alpha\,d_{1/2\,1/2}^{1/2}(\beta)d_{1/2\,1/2}^{1/2}(\tilde{\beta})\\ &\quad+\sin^2\alpha\,d_{1/2\,1/2}^{3/2}(\beta)d_{1/2\,1/2}^{3/2}(\tilde{\beta})\end{aligned} \tag{4.12}$$

and

$$n_{\pi}(\alpha,\beta\tilde{\beta})=\exp[N_{\text{intr}}^{\pi}(\alpha)\cos\beta\cos\tilde{\beta}]\ , \tag{4.13}$$

with $N_{\text{intr}}^{\pi}(\alpha)$ being the average pion number of Eq. (3.30). Altogether Eqs.(4.11)–(4.13) give the norm overlap. Figure 7 displays some norm overlaps at representative values of R and α. Since the intrinsic wave function does not show good positive parity the overlaps are not symmetric around $\pi/2$. For larger values of α they can become negative. The slope of the overlap shows that approximations of Gaussian type are bound to fail. This sheds some unfavorable light on semiclassical quantization procedures, which all work in the small amplitude and therefore Gaussian limit. By similar techniques one obtains the overlap function for the particle number in the pion field:

$$\begin{aligned}N^{\pi}(\alpha,R;\beta\tilde{\beta})&=\langle \bar{\xi},\alpha,R\mid \hat{N}_{\pi}R_y(\beta)R_2(\tilde{\beta})\mid \bar{\xi},\alpha,R\rangle\\ &=N_{\text{intr}}^{\pi}(\alpha,R)\cos\beta\cos\tilde{\beta}\,n(\alpha;\beta\tilde{\beta})\ .\end{aligned} \tag{4.14}$$

This can be used to calculate the number of pions

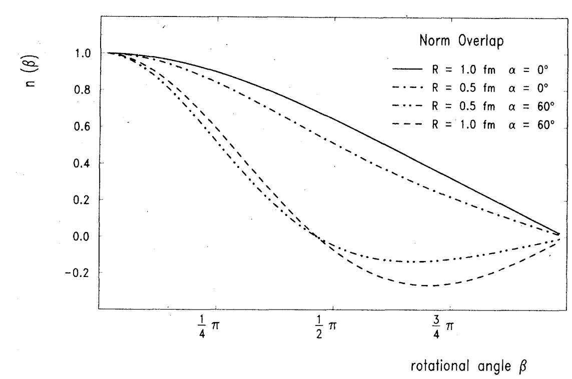

FIG. 7. The norm overlap $n(\alpha,\beta,\tilde{\beta}=0)$ is plotted vs β for the cases $R=0.5$ and 1.0 fm and $\alpha=0°$ and 60°. The parameters used are $B^{1/4}=0.125$ GeV, $Z=1.75$, $g_{\pi NN}=14$ GeV^{-1}, and $\eta_{\pi}=0.2$ fm.

$N_{JT}^{\pi}(\alpha,R)$ in the cloud, which is associated to a projected total state with angular momentum and isospin J and T, respectively. Illustrative numbers will be shown in Fig. 11.

B. Hamiltonian overlap

The Hamiltonian overlap can be written as $h=h_{BN}+h_{\pi}+h_{\rm coupl}$. Using Eqs. (4.5) and (2.6) one gets

$$h_{BN}(\alpha,R;\beta\widetilde{\beta}) =[E_N(R)\cos^2\alpha\, d^{1/2}_{1/2\,1/2}(\beta)d^{1/2}_{1/2\,1/2}(\widetilde{\beta}) +E_{\Delta}(R)\sin^2\alpha\, d^{3/2}_{1/2\,1/2}(\beta)d^{3/2}_{1/2\,1/2}(\widetilde{\beta})]n_{\pi}(\alpha;\beta\widetilde{\beta}) \quad (4.15)$$

and with Eqs. (2.3), (4.8), and the properties (3.3) of coherent states

$$h_{\pi}(\alpha,R;\beta,\widetilde{\beta})=\left[\sum_j\int d^3k\,\omega(k)\xi_j^*(\mathbf{k})\xi_j(\mathbf{k};\beta\widetilde{\beta})\right]\times n_{\pi}(\alpha;\beta\widetilde{\beta})n_{BN}(\alpha;\beta\widetilde{\beta}) \quad (4.16)$$

or by a straightforward calculation, inserting Eqs. (3.18) and (4.10)

$$h_{\pi}(\alpha,R;\beta,\widetilde{\beta})=E^{\pi}_{\rm intr}(\alpha,R)\cos\beta\cos\widetilde{\beta}\,n(\alpha;\beta\widetilde{\beta}) \;. \quad (4.17)$$

The coupling term is obtained by inserting Eq. (2.8) into (4.15) yielding

$$h_{\rm coupl}(\alpha,R;\beta\widetilde{\beta}) =i\int d^3k\,f_R(k)\sum_j\langle BN(\alpha)\,|\,\hat{X}_j(\mathbf{k})\,|\,BN(\alpha;\beta\widetilde{\beta})\rangle \times[\xi_j(\mathbf{k},\beta\widetilde{\beta})-\xi_j^*(\mathbf{k})]n_{\pi}(\alpha;\beta\widetilde{\beta}) \;. \quad (4.18)$$

The explicit evaluation yields

$$h_{\rm coupl}(\alpha,R;\beta\widetilde{\beta})=E^{\rm SE}_{\rm intr}(\alpha,R)n_{\pi}(\alpha;\beta\widetilde{\beta})[A_{3z}(\alpha;\beta\widetilde{\beta})(1+\cos\beta\cos\widetilde{\beta})-A_{3x}(\alpha;\beta\widetilde{\beta})\sin\beta\cos\widetilde{\beta} -A_{1z}(\alpha;\beta\widetilde{\beta})\cos\beta\sin\widetilde{\beta}+A_{1x}(\alpha;\beta\widetilde{\beta})\sin\beta\sin\widetilde{\beta}] \;. \quad (4.19)$$

The derivation and the functions $A_{3z}(\alpha;\beta,\widetilde{\beta})$, etc., are given in Appendix C. Figure 8 shows some Hamiltonian overlaps as representative examples. They have qualitatively a structure similar to the norm overlaps. In both cases one realizes a strong dependence on the value of α, a feature which will have a pronounced effect on the projected energies.

The evaluation of the integrals over β and $\widetilde{\beta}$ is performed by means of a Gauss-Laguerre quadrature with 48 points in the range of $0\le\beta\le\pi$. Some results of the projections are displayed in Fig. 9 for the lowest three states with $I=T$. There the quantity $|\,a_{JT}\,|^2$ is plotted which is with Eq. (3.5) defined as

$$|\,\xi,\alpha\rangle=\sum_{JT}a_{JT}\,|\,\psi_{JT}\rangle \;, \quad (4.20)$$

where $|\,\psi_{JT}\rangle$ are the normalized projected states. Apparently for $\alpha=0$ the intrinsic state consists predominantly of a nucleon, only 15% and less of a Δ, and all other components are negligible. For $\alpha=60°$ the strongest component is the Δ and the nucleon is about 20% only. The curves show some variation with R.

Figure 10 shows the corresponding energies. The intrinsic energy is always surrounded on both sides by projected ones due to the sum rules

$$\sum_{JT}|\,a_{JT}\,|^2=1 \;, \quad (4.21)$$

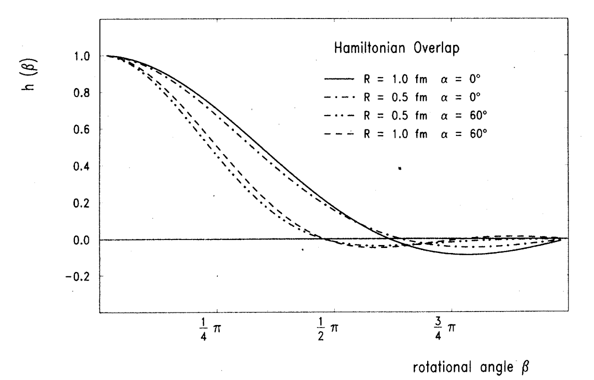

FIG. 8. The Hamiltonian overlap $h(\alpha,\beta,\widetilde{\beta}=0)$ is plotted vs β for the cases $R=0.5$ fm and 1.0 fm and $\alpha=0°$ and 60°. The overlap is normalized to $h(\alpha,\beta=0,\widetilde{\beta}=0)=1$. The parameters used are those of Fig. 7.

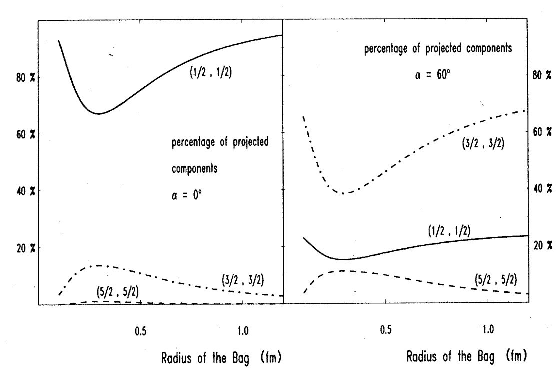

FIG. 9. The percentage of the projected components contained in the intrinsic wave function, i.e., $|\,a_{JT}\,|^2$ of Eq. (4.23) is plotted for various (J,T) values in dependence on the bag radius R. The left figure corresponds to $\alpha=0°$ and the right one to $\alpha=60°$. The parameters used are those of Fig. 7.

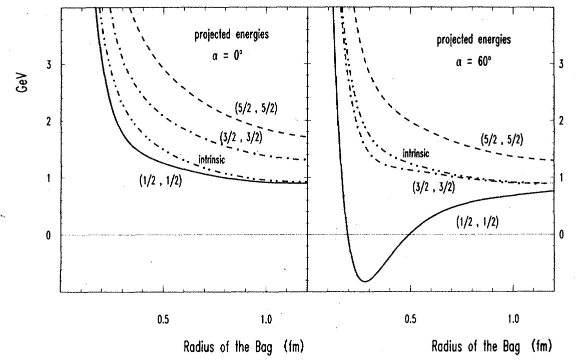

FIG. 10. The projected energies $E_{JT}(\alpha,R)$ are plotted for $\alpha=0°$ (left figure) and $\alpha=60°$ (right figure) vs the bag radius R. The intrinsic energy (dashed-dotted-dotted) is given for comparison. Only (J,T) states with $J=T$ are selected. The parameters used are those of Fig. 7.

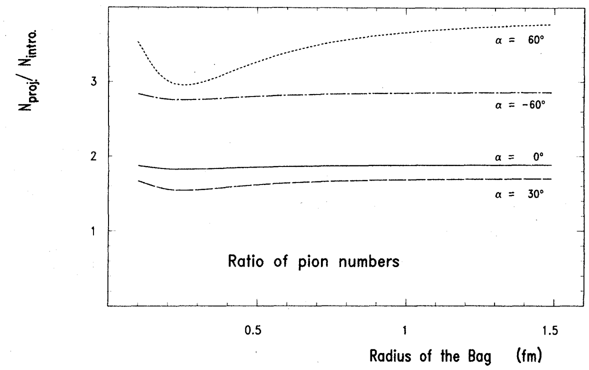

FIG. 11. The ratio of average pion numbers in the projected and intrinsic state. The values are given for various mixing angles α in dependence on R. The curves show that the effect of the projection is strongly α dependent. The parameters used are $B^{1/4}=0.125$ GeV, $g=17$ GeV^{-1}, $Z=1.75$, and $\eta_\pi=0.17$ fm. The projection is performed on $J=T=\frac{1}{2}$.

$$\sum_{JT} |a_{JT}|^2 E_{JT}=E_{\text{intr}} \; . \tag{4.22}$$

Since in the present examples there is always one clearly dominating component the intrinsic energy is closest to the nucleon energy for $\alpha=0$ and closest to the Δ energy at $\alpha=60°$. In both cases these energies basically agree at larger R values where the influence of the pion field is weaker. All numbers apparently are strongly dependent on the value of α. In any case, however, the projected nucleon state is the lowest one and is lower than the intrinsic energy. This shows that the projection cannot provide a mechanism against collapse, a fact which is confirmed by the calculations. One should not be disturbed by the negative energy at small R and $\alpha=60°$ in Fig. 10. The values of the free parameters are not yet fitted to experimental data and no vertex renormalization has been performed.

Actually the average pion number in the projected nucleon state is noticeably larger than in the intrinsic state. This can be seen at Fig. 11 where the ratio of the projected and nonprojected pion numbers is plotted. This ratio is always larger than 1 and shows a strong dependence on α and a somewhat weaker one on R. Thus the effect of the pion cloud is largest in the projected nucleon.

V. VERTEX RENORMALIZATION

The coupling constant $g_{\pi NN}$ of the previous sections has not yet been fixed. Owing to the incorporation of the finite size of the pions in the cloud and due to the angular momentum and isospin projections the $g_{\pi NN}$ should not be equal to the experimental

$$g_{\pi NN}^{\text{expt}}=7.25 \text{ GeV}^{-1} \; . \tag{5.1}$$

For elementary pions and if no Δ states are assumed in the intrinsic bag state the connection is given by[25]

$$g_{\pi NN}\langle \text{model} \,|\, \boldsymbol{\sigma}\cdot\mathbf{k}\tau_j \,|\, \text{model}\rangle = g_{\pi NN}^{\text{expt}}\langle \text{expt} \,|\, \boldsymbol{\sigma}\cdot\mathbf{k}\tau_j \,|\, \text{expt}\rangle \; , \tag{5.2}$$

where $|\text{model}\rangle$ means the projected model wave functions used in this paper and $|\text{expt}\rangle$ means the structureless nucleon state $|\frac{1}{2}\,\frac{1}{2}\rangle$ used for the experimental analysis. This can be written down explicitly, also in the case for intrinsic Δ components, as

$$g_{\pi NN}^{\text{expt}}=p(\alpha)g_{\pi NN} \tag{5.3}$$

with

$$p(\alpha)=\frac{\langle \bar{\xi},\alpha \,|\, P_{JM_J}^{\dagger}P_{TM_T}^{\dagger}\hat{X}_{ij}P_{JM_J}P_{TM_T} \,|\, \bar{\xi},\alpha\rangle\langle \bar{\xi},\alpha \,|\, P_{JM_J}P_{TM_T} \,|\, \bar{\xi},\alpha\rangle^{-1}}{\langle JM_J,TM_T \,|\, \sigma_i\tau_j \,|\, JM_J,TM_T\rangle} \; , \tag{5.4}$$

where $J=T=M_J=M_T=\frac{1}{2}$ and

$$\begin{aligned}\hat{X}_{ij}=&\sum_{st}^{1/2}\sum_{s't'}^{1/2}(\sigma_i)_{ss'}(\tau_j)_{tt'}\hat{v}_{st}^{\dagger}\hat{v}_{s't'}\\&+\left[\frac{72}{25}\right]^{1/2}\sum_{st}^{1/2}\sum_{ST}^{3/2}(S_i)_{Ss}(T_j)_{Tt}\hat{\delta}_{ST}^{\dagger}\hat{v}_{st}\\&+\left[\frac{72}{25}\right]^{1/2}\sum_{st}^{1/2}\sum_{ST}^{3/2}(S_i^{\dagger})_{sS}(T_j^{\dagger})_{tT}\hat{v}_{st}^{\dagger}\hat{\delta}_{ST}\\&+\tfrac{4}{4}\sum_{ST}^{3/2}\sum_{st}^{1/2}(\Sigma_i)_{SS'}(\theta_j)_{TT'}\hat{\delta}_{ST}^{\dagger}\hat{\delta}_{S'T'} \; .\end{aligned} \tag{5.5}$$

We will restrict ourselves to $i=z$ and $j=3$ since the ratio $p(\alpha)$ is independent of the actual choice of indices i and j. The operators of Eq. (5.5) are all tensor operators of first rank. In case of axial symmetry the general formula for the matrix elements of a tensor operator $T_{\kappa\mu}$ between projected states is with $J_z\,|\,\psi\rangle=K_0\,|\,\psi\rangle$ given by[26]

$$\langle \psi \,|\, P_{J'M'}^{\dagger}T_{\kappa\mu}P_{JM} \,|\, \psi\rangle =(-)^{J'-M'}\begin{bmatrix} J' & \kappa & J\\ -M' & \mu & M\end{bmatrix}\langle J'||T_\kappa||J\rangle \tag{5.6}$$

with

$$\langle J'||T_\kappa||J\rangle=\frac{(2J'+1)(2J+1)}{2}\sum_{\mu}\begin{bmatrix} J' & \kappa & J \\ -K_0 & \mu & K_0-\mu \end{bmatrix}\int_0^{\pi} d\beta \sin\beta\, d^{J}_{K_0-\mu,K_0}(\beta)\langle\psi\,|\,T_{\kappa\mu}R_y(\beta)\,|\,\psi\rangle \ . \tag{5.7}$$

If one applies this to spin and isospin one obtains after some algebra

$$\begin{aligned} p(\alpha)=\frac{1}{9N_J}\int d\beta\sin\beta\int d\tilde{\beta}\sin\tilde{\beta}n_\pi(\alpha;\beta\tilde{\beta})[&d^{1/2}_{1/2\,1/2}(\beta)d^{1/2}_{1/2\,1/2}(\tilde{\beta})\langle BN(\alpha)\,|\,\hat{X}_{z3}\,|\,BN(\alpha;\beta\tilde{\beta})\rangle \\ &+d^{1/2}_{-1/2\,1/2}(\beta)d^{1/2}_{1/2\,1/2}(\tilde{\beta})\langle BN(\alpha)\,|\,\hat{X}_{+3}\,|\,BN(\alpha,\beta\tilde{\beta})\rangle \\ &+d^{1/2}_{1/2\,1/2}(\beta)d^{1/2}_{-1/2\,1/2}(\tilde{\beta})\langle BN(\alpha)\,|\,\hat{X}_{z+}\,|\,BN(\alpha,\beta\tilde{\beta})\rangle \\ &+d^{1/2}_{-1/2\,1/2}(\beta)d^{1/2}_{-1/2\,1/2}(\tilde{\beta})\langle BN(\alpha)\,|\,\hat{X}_{++}\,|\,BN(\alpha,p\tilde{p})\rangle] \ . \end{aligned} \tag{5.8}$$

Here, for example, the $\hat{X}_{+3}$ means that in Eq. (5.5) for $\hat{X}_{ij}$ the matrices σ_i, S_i, $S_i^{\dagger}$, Σ_i are to be replaced by σ_+, S_+, $S^{\dagger}_+$, Σ_+ with, e.g., $\Sigma_+=\Sigma_x+i\Sigma_y$. The normalization N_J in Eq. (5.8) is given as

$$N_J=\int_0^{\pi} d\beta\sin\beta\int_0^{\pi} d\tilde{\beta}\sin\tilde{\beta}\, d^{1/2}_{1/2\,1/2}(\beta)d^{1/2}_{1/2\,1/2}(\tilde{\beta})n(\alpha;\beta\tilde{\beta}). \tag{5.9}$$

Inserting in Eq. (5.8) the $|\,BN(\alpha,\beta\tilde{\beta})\rangle$ from Eq. (4.5) and using the matrices from Appendix A yields the final expression for $p(\alpha)$ given in Appendix D.

One has to take into account that $g_{\pi NN}$ has been modified into an effective $g_{\text{eff}}(R)$ due to the finite pion size and that the $p(\alpha)$ depends on the $g_{\text{eff}}(R)$ since this enters in the evaluation of $n_\pi(\alpha;\beta\tilde{\beta})$. [See Eqs. (4.15) and (3.31), with $g_{\pi NN}$ replaced by g_{eff}.] Thus the equation for the vertex renormalization reads explicitly

$$g^{\text{model}}_{\pi NN}=g_{\pi NN}\left[1+2C_3\left[\frac{n_\pi}{R_0}\right]^2\right]^{-3/2} p(\alpha_0)=g^{\text{expt}}_{\pi NN} \ . \tag{5.10}$$

This is a nonlinear equation which has to be fulfilled for the model state of the nucleon, i.e., at a bag radius R_0 and a mixing factor α_0 where both correspond to the minimum of the projected energy valley $E^{(R)}_{JT}(\alpha)$ with $J=T=\frac{1}{2}$.

VI. SELF-CONSISTENT SOLUTIONS OF THE NUCLEON

In the preceding section we described how to perform a proper renormalization of the pion-nucleon vertex in order to obtain the $g_{\pi NN}$. There are, however, two other unknown parameters in the present model: the volume energy B and the center-of-mass and cavity correction Z, both in Eq. (2.15). There are no reliable QCD calculations which give precise values for these quantities and therefore they are here considered as adjustable parameters in order to obtain a proper mass of the proton ground state. Hence in the three-dimensional parameter space (i.e., $g_{\pi NN},B,Z$) values varied such that the corresponding minima α_0 and R_0 of the projected energy curve $E_{1/2\,1/2}(\alpha,R)$, yield the proper $g^{\text{expt}}_{\pi NN}$ and the nucleon energy of 0.938 GeV. In practice the search is done by the computer which looks for the zeros of the function

$$f(g_{\pi NN},B,Z)=\left[\frac{E_{1/2\,1/2}(\alpha_0,R_0)}{0.938}-1\right]^2+\left[\frac{g^{\text{model}}_{\pi NN}}{g^{\text{expt}}_{\pi NN}}-1\right]^2 . \tag{6.1}$$

The results of this procedure are described in this section as an application of the present formalism. Since the size of the pions in the cloud is unknown, we perform the searching for all values of n_π between 0.17 and 0.3 fm. The interesting feature which comes out is that for each n_π there exist two sorts of solutions: one corresponding to the MIT bag with a rather weak pion field, i.e., some sort of cloudy bag, and the other corresponding to a small bag of $R\simeq 0.3$–0.5 fm surrounded by a strong pion field. The latter solution bears some similarity to the so-called little bag.

For $\eta_\pi=0.24$ fm the properties of these two solutions are presented in detail in Figs. 12–14. As shown in Fig. 12 in both cases the $(\frac{3}{2},\frac{3}{2})$ component is the largest one in

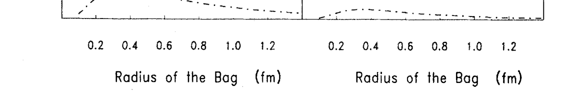

FIG. 12. The percentage of the projected components is plotted for the little-bag solution and MIT-bag (cloudy-bag) solution vs the bag radius R. The radius of the pion is assumed to be $\eta_\pi=0.24$ fm. The self-consistently determined parameters are $g_{\pi NN}=13.59\ \text{GeV}^{-1}$, $B^{1/4}=0.233$ GeV, $Z=0.587$, $\alpha_0=55.44°$, $R_0=0.412$ fm for the little bag, and $g_{\pi NN}=7.871\ \text{GeV}^{-1}$, $B^{1/4}=0.124$ GeV, $Z=1.404$, $\alpha_0=55.8°$, $R_0=1.185$ fm.

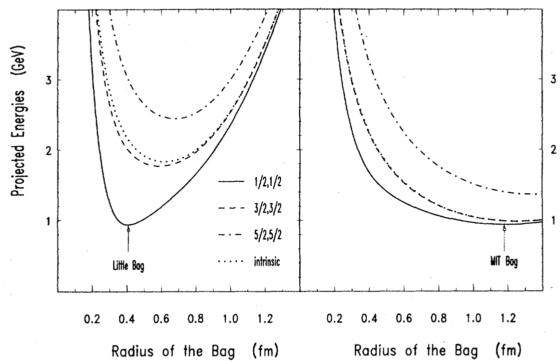

FIG. 13. The projected energies for the little-bag and MIT-bag (cloudy-bag) solutions are plotted vs the bag radius R for $\eta_\pi=0.24$ fm. The intrinsic energy is also indicated by a dotted line. For the MIT bag the intrinsic solution is very close to the projected $\frac{3}{2},\frac{3}{2}$ solution. The parameters are those of Fig. 12.

the intrinsic solution, the $(\frac{1}{2},\frac{1}{2})$ component, to which the solution is optimized, is smaller than 30% in general. This is due to the fact that the Δ-π coupling is stronger than the N-π coupling. The projected energies are shown in Fig. 13. There the minimum of the little-bag solution is well pronounced whereas the curve for the MIT bag is

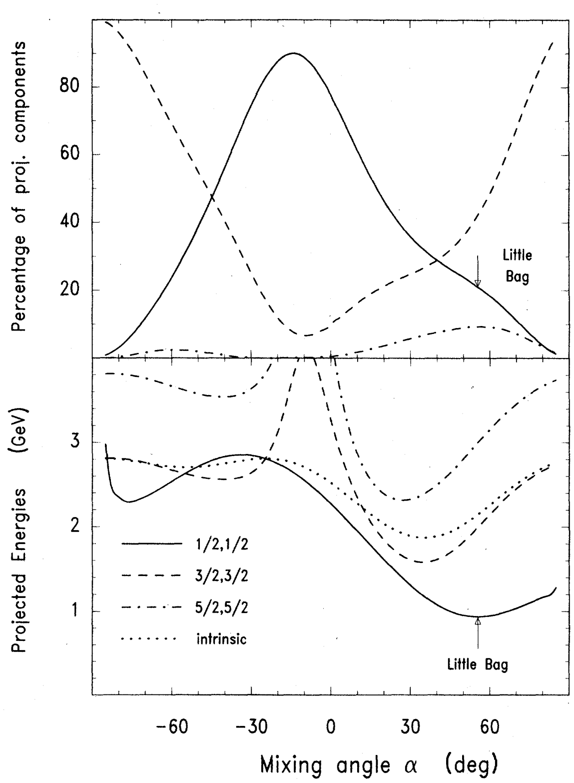

FIG. 14. The percentage of the projected components and the corresponding energies are plotted vs α for the self-consistent radius $R=0.412$ fm corresponding to a little bag and a pion radius of $\eta_\pi=0.24$ fm. The intrinsic energy is given for comparison and indicated by the dotted line. The parameters are those of Fig. 12.

rather flat. In the present model the latter solution ought to be improved by mixing wave functions with different R, from which, perhaps, also a description of the Roper resonance could arise. The minima for the Δ resonance are at slightly larger bag radii than for the nucleon, for the little-bag solution the difference is about 0.2 fm. However, in neither solution the experimental N-Δ splitting is reproduced. For this one probably needs a better intrinsic wave function (see discussion below) and a proper treatment of the one-gluon-exchange interaction. For the little-bag solution the variation of the percentage of projected components and of the energies versus α is given in Fig. 14. Again one finds that the Δ minimum is at a different α value compared to the nucleon minimum. For small values of α the nucleon component dominates. At $\alpha\cong-25°$ the $G(\alpha)$ vanishes and hence also the pion field. There the projected nucleon and Δ are degenerate. Furthermore the percentage of the $(\frac{5}{2},\frac{5}{2})$ component goes to zero with diverging energy. Since for the little-bag solution the minima of the energies of the nucleon and the Δ occur at noticeably different R and α values, one has to conclude that, at least in the presence of strong fields, the projections have to be performed before the variation.

Before we discuss the physical relevance of the above model results and before we show some clear conclusion we prefer to present some more details of the solutions obtained for a range of η_π. The resulting radii of the bag can be seen in Fig. 15 as a function of η_π. The dashed parts of the curve, corresponding to the little-bag solution, indicate regions of the parameters, where the self-consistency condition can only be fulfilled to $\leq 5\%$. One realizes that several solutions fulfill that. However, in many aspects they are rather similar to each other and need not be discussed separately. Apparently for little-bag solutions we have $0.3 \leq R \leq 0.5$ fm depending on the value of η_π. The solutions with the weak pion field, here called MIT solutions, all have a radius of $R\approx1.2$ fm.

The values of the volume energy parameter $B^{1/4}$ for the

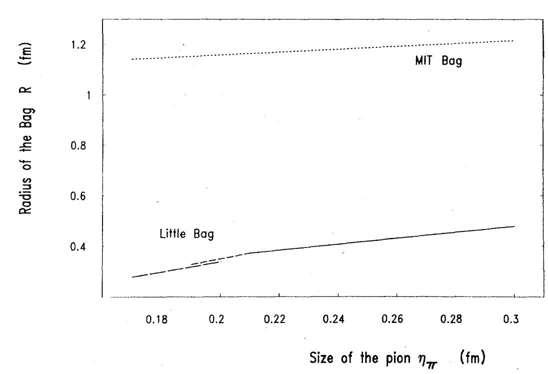

FIG. 15. For a range of pion radii η_π the bag radii of the self-consistent solutions are plotted. Two sorts of solutions exist: One, corresponding to a cloudy bag or an MIT bag with $R\approx1.2$ fm and small pion corrections (dotted line), and another one with small-bag radii around $R\approx0.4$ fm with a strong pion field. The dashed parts of the little-bag curve indicate that the self-consistency condition was only fulfilled to 5%. The parameters resulting from the self-consistency procedure can be extracted from the other figures.

various solutions can be extracted from Fig. 16. Since little-bag solutions are associated with small R they are not very sensitive to a variation of B. Thus from the pure minimization of Eq. (6.1) one would obtain in certain η_π regions even negative values of B. In the present calculation they are suppressed by allowing only variations of B with $B^{1/4} \geq 0.1$ GeV. For small R, where it is applied, this restriction has only little effect on the volume energy $(4\pi/3)BR^3$. The little-bag solutions require for larger η_π a $B^{1/4}$ around 0.22 GeV, a value which is also given by Carlson, Hansen, and Peterson[28]. The MIT bag shows a $B^{1/4}$ around 0.125 GeV close to the MIT value of DeGrand, Jaffe, Johnson, and Kiskis[29] of $B^{1/4}=0.145$ GeV.

The little-bag solutions require a strong renormalization of the coupling constant as one can see at Fig. 17. Whereas for the MIT solution the $g_{\pi NN}$ is close to the experimental value of 7.25 GeV^{-1} the corresponding value for the little-bag solution is about twice that much. This effect comes only to 20% from the projection and to 80% from the finite size of the pion, as is demonstrated in Fig. 18, where the $p(\alpha)$ is plotted. Actually the self-consistent α values are about 66° for the large bag and between 50° and 60° for the little-bag solution.

The values of Z of Eq. (2.15), corresponding to center-of-mass and cavity corrections, are given for the self-consistent solutions in Fig. 19. For smaller pion radii η_π one needs negative values of Z for the little bag in order to reach self-consistency. Here the two coexisting solutions for the little bag show noticeably different values for Z. As long as there does not exist a firm theory for Z one has to accept it.

The average pion numbers for the self-consistent solutions are shown in Fig. 20. The MIT bag has about 0.15 pions in the cloud, more or less independent of the pion radius η_π. The little-bag solutions, on the contrary, show a noticeable η_π dependence with values between 2 and 4. A similar trend is seen from the self-energy given in Fig. 21, which for the MIT bag is rather small, about -0.3 GeV, whereas it varies for the little bag between -1 and -6 GeV. The pion number and the self-energy demonstrate that the solutions obtained have indeed some features presently frequently discussed:[13] One corresponds to the MIT bag with little pion-field corrections,[8,11,12] and the other to a little bag with strong pion-field corrections.[9,10]

It remains to discuss the physical relevance of our results. From fundamental points of view there are probably no basic objections against the parameters emerging from our self-consistent procedure in case of the little bag. However, the fact that we use a linearized Lagrangian is inconsistent with the appearance of rather strong pion fields. Thus one should take our results as a hint for the possible existence of little-bag solutions but by no means as a proof. If, furthermore, the mechanism to stabilize the nucleon against collapse is not given by the finite size of the pion, as it is assumed here, the behavior of the solu-

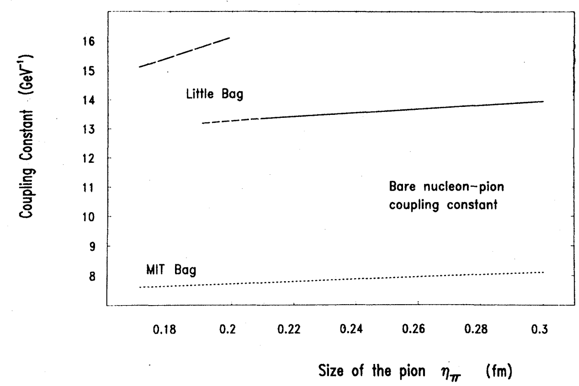

FIG. 17. The pion—bare-nucleon coupling constant $g_{\pi NN}$ for the self-consistent solutions as a function of the pion radius η_π. The dashed parts of the little-bag solutions indicate regions where the self-consistency condition cannot be fulfilled exactly but up to 5%. All curves incorporate angular momentum and isospin projection on the proton ground state.

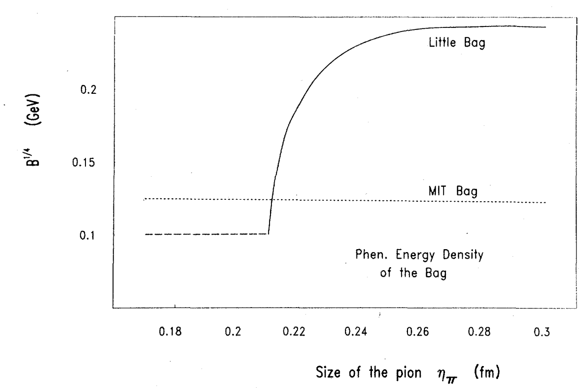

FIG. 16. For a range of pion radii η_π the fitted volume energy parameter $B^{1/4}$ is plotted for the little-bag solutions and the MIT-bag (cloudy-bag) solution. The variation of $B^{1/4}$ has been limited to values of $B^{1/4} \geq 0.1$ GeV. The dashed part of the little-bag curve indicates a region where the self-consistency condition cannot be fulfilled exactly but only to $\leq 5\%$. All curves incorporate angular momentum and isospin projection on the proton ground state.

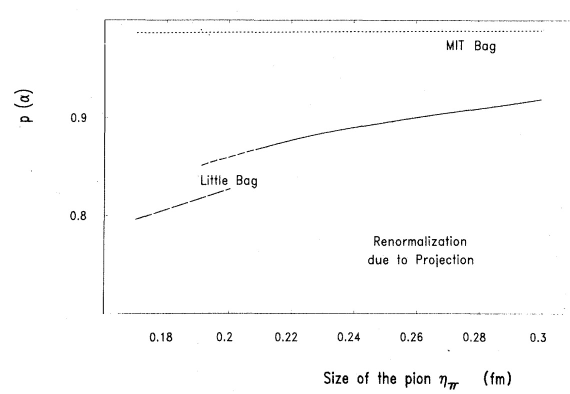

FIG. 18. The renormalization factor of the pion—bare-nucleon coupling constant due to the angular momentum and isospin projection. The values are given for the self-consistent solutions as a function of the pion radius η_π. Dashed parts indicate regions where the self-consistency condition can be satisfied only up to 5%.

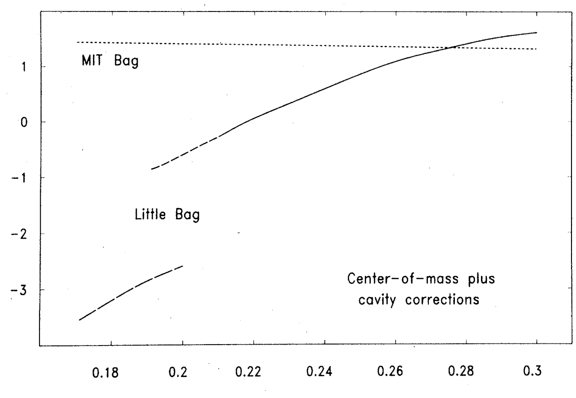

FIG. 19. The center-of-mass and cavity correction Z of the MIT-bag and little-bag energy is given for the self-consistent solutions as a function of the pion radius η_π. Dashed parts indicate regions of η_π where the self-consistency condition can only be satisfied up to 5%.

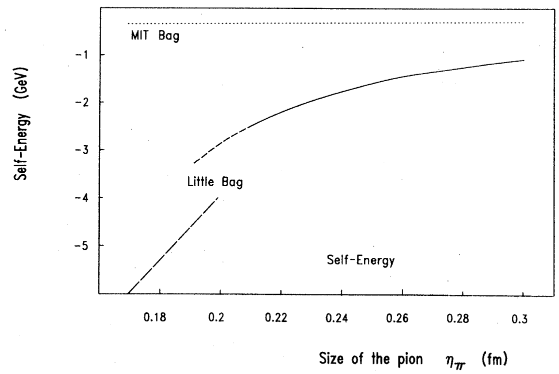

FIG. 21. The self-energy of the self-consistent little-bag and MIT-bag (cloudy-bag) solutions as a function of the pion radius η_π. Dashed regions indicate where the self-consistency condition can be satisfied only up to 5%.

tions at small R may be quite different.

One could obtain some more insight into the properties of both sorts of solutions, if one calculated observable quantities as electromagnetic rms radii, charge distributions, magnetic moments, etc. However, even in the case of the MIT bag solution we did not do it because of the following reason: The present theory is a variational theory and hence its results are as good as its trial function. In order to investigate the projection techniques we restricted ourselves to trial wave functions axially symmetric in both spin and isospin space. The use of a more general trial function, having, e.g., a hedgehog structure, would result in a noticeably larger self-energy and hence, in a variational sense, a better solution: a hedgehog corresponds to assuming the three quarks in the spin-flavor state given by $(|u\downarrow\rangle - |d\uparrow\rangle)^3$. Written in terms of colorless baryonic states this yields the intrinsic bare nucleon wave function:

$$|BN(hh)\rangle = \sum_J^{1,2,3/2} \sum_K \frac{1}{[2(2J+1)]^{1/2}} (-)^{J-K} \times |J,K;T=J,T_3=-K\rangle \,.$$

A comparison of the intrinsic self-energy (3.20) at the maximum of $G^2(\alpha)$ with the corresponding hedgehog self-energy of Ref. 30 shows that one gains exactly a factor of 3 by using the hedgehog. [For a comparison one should take into account that the pion source $\rho_R(k)$ in Ref. 30 differ by a factor of 3.] Furthermore it has been shown[30] that without projections the hedgehog configuration minimizes the energy of the cloudy-bag Hamiltonian and is therefore a much better trial wave function than the present one, in which, for example, only neutral pions are coupled to the quarks. This is the reason why observables like rms radii, etc., have not been evaluated and why we did not improve the approach by one-gluon exchanges. This is also the reason why a comparison with the results of other models is of limited value. However, the use of a hedgehog configuration will complicate the projection procedure, a problem which will be studied separately.

There is, however, one firm conclusion which can be drawn from the present investigation and which is illustrated by Fig. 13 and particularly Fig. 22. Whereas for the energy of the MIT-bag solution the effect of the projection is rather small this is not so for the little-bag solution. There the gain in energy is of the order of 1 GeV or more. Thus an investigation of little-bag solutions without projection on the proper quantum numbers, for example, in a purely classical picture or using the hedgehog ansatz, can lead to wrong results. Furthermore the minima of the intrinsic and projected solutions are at quite different R values from which one must conclude that even a projection before the variation, i.e., a variation with wave functions already projected on good J and T quantum numbers, is required for a proper description of little-bag solutions.

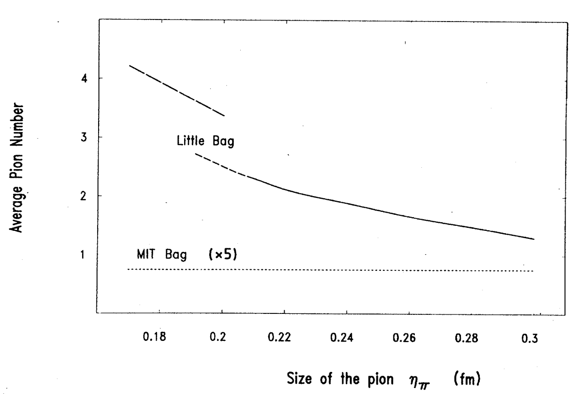

FIG. 20. The average pion number of the self-consistent little-bag and MIT-bag (cloudy-bag) solutions in dependence on the pion radius η_π. Dashed regions indicate where the self-consistency condition can be satisfied only up to 5%. The values of the MIT bag (cloudy bag) are enlarged by a factor 5. There are in reality about 0.15 pions per nucleon.

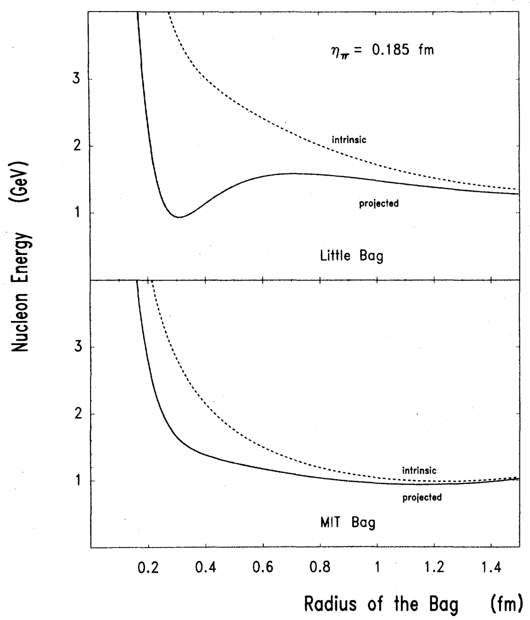

FIG. 22. The energy of the little-bag solution and the MIT-bag (cloudy-bag) solution is given for the pion radius $\eta_\pi = 0.185$ fm vs the bag radius R. Actually only the minima of the $\frac{1}{2}, \frac{1}{2}$ projected curves are self-consistent. The self-consistently determined parameters are $g_{\pi NN} = 15.605$ GeV^{-1}, $B^{1/4} = 0.1$ GeV, $Z = -3.00$, $\alpha_0 = 50.89°$, $R_0 = 0.309$ fm, and $g_{\pi NN} = 7.67$ GeV^{-1}, $B^{1/4} = 0.125$ GeV, $Z = 1.473$, $\alpha_0 = 66.55°$, and $R_0 = 1.157$ fm for the little-bag and the MIT-bag solution, respectively.

VII. SUMMARY, CONCLUSION, AND OUTLOOK

The present paper suggests a variational quantum-field-theoretical approach (VQF) to the chiral bag which is characterized by two properties. First, it is a variational model working with field operators and assuming the boson field wave functions to be coherent states. The state of the quark-core (bag) is properly parametrized, in the present case as a mixture between a bare nucleon state and a bare Δ-isobaric state. Second, the approach is fully quantum mechanical since the total object, quark core plus pion cloud, is projected on good total spin and isospin. The collapse of the nucleon is prevented by the finite extension of the pions.

The VQF approach is formulated here with the pion field coupled to the quark core on its surface. It can be extended, however, to include other interaction mechanisms and other boson fields, e.g., the ω- and ρ-meson, which, if necessary, can also be treated with a finite extension. The theory can also be applied to the chiral-soliton models. It only requires, in addition, to approximate the σ field, which replaces the bag confinement, by a coherent state and to parametrize the quark wave functions in a way suitable for a variational treatment. Compared to the usual treatments this would have the advantage that one can introduce quantum corrections in a clear way. (While this paper was revised, a paper by M. C. Birse [University of Washington report, 1985 (unpublished)] came to our attention, in which this projection formalism has been applied to the linear chiral σ model.)

In this paper the VQF approach has been applied to the energy of the nucleon ground state. For other properties and for excited states as, e.g., the physical Δ or the Roper resonance it might be advisable to use an intrinsic bare nucleon state which is better suited and has more degrees of freedom. A frequently discussed candidate for that is the so-called "hedgehog" solution which implies a particularly structured pion field. It is actually no problem to incorporate these sorts of states into the present formalism. The theory can even be used to give a foundation for the hedgehog, which has been investigated more in detail in a separate publication.[30] The use of such states introduces triaxial components to the total wave function in spin and isospin space. However the ensuring complications in the projection procedure are only of a technical nature.

With a rather simple trial wave function the VQF model has been applied to the ground state of the nucleon with the result that two sorts of solutions exist, one corresponding to the MIT bag with a weak pion field, i.e., some sort of cloudy bag, the other corresponding to a bag with a radius of $R \simeq 0.3-0.5$ fm and a strong pion field. Both solutions have in the present model the same right of existence insofar as they yield the same nucleon energy and the same pion-nucleon vertex. They do correspond, however, to different values of the parameters B, $g_{\pi NN}$, and Z, which are treated as fitting parameters. Subject to these parameters the present numbers should be taken as a hint for the possible existence of little-bag solutions no matter which radius of the pion is assumed. Of course, a more conclusive theoretical evidence for little bags requires aside from additional information on these parameters a fully nonlinear treatment of the pion-bag interaction. Furthermore, some more properties of the nucleon such as rms radii and magnetic moments should be investigated using a better trial wave function. However one point should be stressed about the present results. The little bag appears as a self-consistent solution of our Lagrangian only if one takes properly into account quantum corrections to the mean-field approximation by the Peierls-Yoccoz projection technique. The present numbers suggest even the use of a projection procedure before the variation.

In conclusion it is evident that basic and challenging problems remain in the application of the present variational quantum-field-theoretical approach to chiral-bag and soliton models. However the potentiality of the model and the success of the first calculations justify continuing effort on both the conceptual and technical aspects of the theory.

ACKNOWLEDGMENTS

J.N.U. would like to thank the Kernforschungsanlage Jülich for support and hospitality and acknowledges a grant from the Deutscher Akademischer Austauschdient. The authors would like to thank M. Harvey, M. Rho, D. Schütte, and W. Weise for illuminating discussions. This research was supported in part by the NATO Scientific Affairs Division under Ref. No. RG.85/0217.

APPENDIX A: ELIMINATION OF QUARK DEGREES OF FREEDOM

This appendix derives Eq. (2.8), which to some extent can already be found in Ref. 6. Because some of the formulas are needed in another context in the present paper the derivation will be given in detail.

Since we deal with nucleon and Δ states, which all have the same orbital wave functions

$$q(\mathbf{r})=\frac{N}{\sqrt{4\pi}}\begin{bmatrix} j_0\left[\dfrac{\Omega r}{R}\right] \\ ij_1\left[\dfrac{\Omega r}{R}\right]\boldsymbol{\sigma}\cdot\mathbf{r}\end{bmatrix}u \tag{A1}$$

the integration over r in Eq. (2.7) can be done separately. Here $\Omega=2.04$ and R is the bag radius. The normalization

$$N^2=\frac{\Omega^3}{2R^3(\Omega-1)\sin^2\Omega} . \tag{A2}$$

The γ_0 and γ_5 are taken in the representation

$$\gamma_0=\begin{bmatrix}1 & 0\\ 0 & -1\end{bmatrix},\quad \gamma_5=\begin{bmatrix}0 & 1\\ 1 & 0\end{bmatrix} . \tag{A3}$$

Then the part of Eq. (2.7) proportional to $a_j(k)$ of the pion field can explicitly be written as

$$\begin{aligned}\frac{2iN^2}{4\pi}\int r^2dr\sin\vartheta\, d\vartheta\, d\varphi\, j_0\left[\frac{\Omega r}{R}\right]j_1\left[\frac{\Omega r}{R}\right]\\ \times(\sigma'_x\sin\vartheta\cos\varphi+\sigma'_y\sin\vartheta\sin\varphi+\sigma'_z\cos\vartheta)\\ \times\tau_j\exp(ikr\cos\vartheta)\delta(r-R)\end{aligned} \tag{A4}$$

if one performs the integration over $\mathbf{r}$ in a coordinate system with the z axis aligned along $\mathbf{k}$. The prime at the spin matrices indicates that they refer to this coordinate system.

Since we have

$$\frac{i}{2}\int_0^{\pi}d\vartheta\cos\vartheta\sin\vartheta\exp(ikr\cos\vartheta)=j_1(kr) \tag{A5}$$

one obtains with $j_0{}^2(\Omega)=j_1{}^2(\Omega)$ and $j_0(\Omega)j_1(\Omega)=\Omega^{-2}\sin^2\Omega$ together with the N of Eq. (A2) an expression identical to (A4) being

$$\frac{\Omega}{\Omega-1}\frac{j_1(kR)}{kR}\boldsymbol{\sigma}\cdot\mathbf{k}\tau_j , \tag{A6}$$

where we have used $k\sigma'_z=\boldsymbol{\sigma}\cdot\mathbf{k}$. Thus the interaction Hamiltonian can be written in the form of Eq. (2.8) and Eq. (2.12) with, e.g.,

$$\hat{X}_j^{\pi N\Delta}(\mathbf{k})=\left\langle\Delta^+_{1/2}\left|\sum_{a=1}^{3}\sigma^a\cdot\mathbf{k}\tau_j^a\right|N^+_{1/2}\right\rangle\hat{\delta}^{\,+}_{1/2\,1/2}\hat{\nu}_{1/2\,1/2} . \tag{A7}$$

Here $|N^+_{1/2}\rangle$ means a nucleon wave function with spin z component equal to $\frac{1}{2}$ and isospin 3 component equal to $\frac{1}{2}$ in a quark representation as, for example, given in Eqs. (B5) and (B7) of Appendix B of Ref. 27:

$$|N^+_{1/2}\rangle=\frac{-1}{\sqrt{18}}\{u\downarrow u\uparrow d\uparrow+u\uparrow u\downarrow d\uparrow+d\uparrow u\downarrow u\uparrow+u\downarrow d\uparrow u\uparrow+d\uparrow u\uparrow u\downarrow+u\uparrow d\uparrow u\downarrow-2d\downarrow u\uparrow u\uparrow-2u\uparrow d\downarrow u\uparrow-2u\uparrow u\uparrow d\downarrow\} ,$$

$$|\Delta^+_{1/2}\rangle=\tfrac{1}{3}\{d\downarrow u\uparrow u\uparrow+u\downarrow d\uparrow u\uparrow+u\downarrow u\uparrow d\uparrow+d\uparrow u\downarrow u\uparrow+u\uparrow d\downarrow u\uparrow+u\uparrow u\downarrow d\uparrow+d\uparrow u\uparrow u\downarrow+u\uparrow d\uparrow u\downarrow+u\uparrow u\uparrow d\downarrow\} .$$

To transform Eq. (A7) to nucleon and Δ degrees of freedom, i.e., eliminating their quark structure, requires the spin and isospin matrices in representations associated to total $t,j=\frac{3}{2}$ states and in mixed representations. They are explicitly given here since they are used several times in this paper: With $j=1,2,3$ or $j=X,Y,Z$ we have

$$(\sigma_j)_{tt'}=(\tau_j)_{tt'}=\begin{array}{c} \\ \tfrac{1}{2}\\ -\tfrac{1}{2}\end{array}\!\!\begin{array}{c}\begin{array}{cc}\quad\tfrac{1}{2}\quad & \quad-\tfrac{1}{2}\quad\end{array}\\ \begin{bmatrix}\delta_{j3} & \delta_{j1}-i\delta_{j2}\\ \delta_{j1}+i\delta_{j2} & -\delta_{j3}\end{bmatrix}\end{array} ,$$

$$(S_j)_{Tt}=(T_j)_{Tt}=\begin{array}{c} \\ \tfrac{3}{2}\\ \tfrac{1}{2}\\ -\tfrac{1}{2}\\ -\tfrac{3}{2}\end{array}\!\!\begin{array}{c}\begin{array}{cc}\qquad\tfrac{1}{2}\qquad & \qquad-\tfrac{1}{2}\qquad\end{array}\\ \begin{bmatrix}-(\tfrac{1}{2})^{1/2}(\delta_{j1}-i\delta_{j2}) & 0\\ (\tfrac{2}{3})^{1/2}\delta_{j3} & -(\tfrac{1}{6})^{1/2}(\delta_{j1}-i\delta_{j2})\\ (\tfrac{1}{6})^{1/2}(\delta_{j1}+i\delta_{j2}) & (\tfrac{2}{3})^{1/2}\delta_{j3}\\ 0 & (\tfrac{1}{2})^{1/2}(\delta_{j1}+i\delta_{j2})\end{bmatrix}\end{array} ,$$

$$(\Sigma_j)_{TT'}=(\theta_j)_{TT'}=\begin{array}{c} \\ \tfrac{3}{2}\\ \tfrac{1}{2}\\ -\tfrac{1}{2}\\ -\tfrac{3}{2}\end{array}\!\!\begin{array}{c}\begin{array}{cccc}\qquad\tfrac{3}{2}\qquad & \qquad\tfrac{1}{2}\qquad & \qquad-\tfrac{1}{2}\qquad & \qquad-\tfrac{3}{2}\qquad\end{array}\\ \begin{bmatrix}\tfrac{3}{2}\delta_{j3} & \tfrac{1}{2}\sqrt{3}(\delta_{j1}-i\delta_{j2}) & 0 & 0\\ \tfrac{1}{2}\sqrt{3}(\delta_{j1}+i\delta_{j2}) & \tfrac{1}{2}\delta_{j3} & (\delta_{j1}-i\delta_{j2}) & 0\\ 0 & (\delta_{j1}+i\delta_{j2}) & -\tfrac{1}{2}\delta_{j3} & \tfrac{1}{2}\sqrt{3}(\delta_{j1}-i\delta_{j2})\\ 0 & 0 & \tfrac{1}{2}\sqrt{3}(\delta_{j1}+i\delta_{j2}) & -\tfrac{3}{2}\delta_{j3}\end{bmatrix}\end{array} .$$

Inserting these matrix elements and the explicit quark wave functions one obtains the well-known formulas [there should be a minus sign in front of the right-hand side of Eq. (B12) of Ref. 27]:

$$\frac{g_{\pi NN}}{g_{\pi q}}=\frac{\langle N^+_{1/2}\mid \sum_a \sigma_i^a\tau_j^a \mid N^+_{1/2}\rangle}{\langle N^+_{1/2}\mid \sigma_i\tau_j \mid N^+_{1/2}\rangle}=\frac{5}{3}\,, \tag{A8a}$$

$$\frac{g_{\pi\Delta N}}{g_{\pi q}}=\frac{\langle \Delta^+_{1/2}\mid \sum_a \sigma_i^a\tau_i^a \mid N^+_{1/2}\rangle}{\langle \Delta^+_{1/2}\mid S_iT_j \mid N^+_{1/2}\rangle}=2\sqrt{2}\,, \tag{A8b}$$

$$\frac{g_{\pi\Delta\Delta}}{g_{\pi q}}=\frac{\langle \Delta^+_{1/2}\mid \sum_a \sigma_i^a\tau_j^a \mid \Delta^+_{1/2}\rangle}{\langle \Delta^+_{1/2}\mid \Sigma_i\theta_j \mid \Delta^+_{1/2}\rangle}=\frac{4}{2}\,, \tag{A8c}$$

with $g_{\pi q}=\Omega/[6f(\Omega-1)]$. These ratios are independent of the particular choice of i and j. Inserting Eqs. (A8) and (A7), and its analogs for the other 3-quark configurations considered, into Eq. (2.8) gives immediately Eqs. (2.13) and (2.14). Thus the coupling Hamiltonian with bag degrees of freedom is known.

As one can see from Eq. (2.13) we will always need in the following the matrices $\boldsymbol{\sigma}\cdot\mathbf{k}$, $\mathbf{S}\cdot\mathbf{k}$, etc. They can be easily obtained from the above matrices by replacing

$$\delta_{j1}\rightarrow k_x,\quad \delta_{j2}\rightarrow k_y,\quad \delta_{j3}\rightarrow k_z\,. \tag{A9}$$

APPENDIX B: PIONS WITH FINITE SIZE

If one inserts the approximations Eq. (2.20) into the Hamiltonian density $\mathscr{H}_{\text{coupl}}(\mathbf{r})$ of Eq. (2.4) with point pions one obtains with $g_{\pi q}=i/(2f)$

$$\mathscr{H}_{\text{coupl}}(\mathbf{r})=-\frac{N^2C_2}{4\pi R}g_{\pi q}\exp\left[-2C_3\left[\frac{r}{R}\right]^2\right]\left[1-C_1\left[\frac{r}{R}\right]^2\right]\sum_{aj}u_a^\dagger\sigma^a\cdot\mathbf{r}\tau_j^a u_a\hat{\phi}_j(\mathbf{r})\delta(r-R)\,. \tag{B1}$$

Inserting now Eq. (2.20) into the interaction Hamiltonian density with finite-sized pions, Eq. (2.17) yields after some calculations

$$\begin{aligned}\mathscr{H}^{\text{mod}}_{\text{coupl}}(r)=-g_{\pi q}\frac{C_2}{R}\frac{N^2}{8\pi}(\pi\eta_\pi{}^2)^{-3/2}\sum_a u_a\int d^3\eta\exp\left[-\frac{C_3}{R^2}[(\mathbf{r}-\boldsymbol{\eta})^2+(\mathbf{r}-\boldsymbol{\eta})^2]\right]&\\ \times\left[\boldsymbol{\sigma}_a\cdot(\mathbf{r}+\mathbf{n})\left[1-\frac{C_1}{R^2}(\mathbf{r}-\boldsymbol{\eta})^2\right]\right.&\\ \left.+\boldsymbol{\sigma}_a\cdot(\mathbf{r}-\boldsymbol{\eta})\left[1-\frac{C_1}{R^2}(\mathbf{r}+\boldsymbol{\eta})^2\right]\right]\tau_j^a\hat{\phi}_j(\mathbf{r})u_a\delta(r-R)&\end{aligned} \tag{B2}$$

which can be simplified to

$$\begin{aligned}\mathscr{H}^{\text{mod}}_{\text{coupl}}(\mathbf{r})=-g_{\pi q}\frac{C_2}{R}\frac{N^2}{4\pi}(\pi\eta_\pi{}^2)^{-3/2}\sum_a u_a\int d^3\eta\exp\left[-\eta^2\left[\frac{2C_3}{R^2}+\frac{1}{\eta_\pi{}^2}\right]\right]&\\ \times\left[\left[1-C_1\frac{r^2}{R^2}\right]\boldsymbol{\sigma}_a\cdot\mathbf{r}+\frac{2C_1}{R^2}\boldsymbol{\eta}\cdot\mathbf{r}\boldsymbol{\eta}\cdot\boldsymbol{\sigma}_a-\frac{C_1}{R^2}\boldsymbol{\sigma}_a\cdot\mathbf{r}\eta^2\right]&\\ \times\tau_j^a\hat{\phi}_j(\mathbf{r})u_a\delta(r-R)\exp\left[-\frac{2C_3}{R^2}r^2\right]\,.&\end{aligned} \tag{B3}$$

For the integration one needs now some symmetry properties which are frequently used also in other places in this paper:

$$\begin{aligned}&\int d^3\eta\, f(\eta^2)\eta_x=\int d^3\eta\, f(n^2)\eta_x\eta_y=0\,,\\ &\int d^3\eta\, f(\eta^2)\eta_x{}^2=\tfrac{1}{3}\int d^3\eta\, f(\eta^2)\eta^2\,.\end{aligned} \tag{B4}$$

The explicit evaluation of the integrals yields then

$$\mathscr{H}^{\text{mod}}_{\text{coupl}}(\mathbf{r})=M(\eta_\pi,R,r)\mathscr{H}_{\text{coupl}}(\mathbf{r}) \tag{B5}$$

with $M(\eta_\pi,R,r)$ given in Eq. (2.22).

APPENDIX C: ANGULAR MOMENTUM AND ISOSPIN PROJECTIONS

This appendix derives Eq. (4.13). Since the matrices for a rotation of the ordinary vector space around the y axis will be used often we list them here for completeness ($i,j=x,y,z$ or 1,2,3)

$$\begin{aligned}R_y(\beta)&=\begin{bmatrix}\cos\beta & 0 & -\sin\beta\\ 0 & 1 & 0\\ \sin\beta & 0 & \cos\beta\end{bmatrix},\\ R_y{}^{-1}(\beta)&=\begin{bmatrix}\cos\beta & 0 & \sin\beta\\ 0 & 1 & 0\\ -\sin\beta & 0 & \cos\beta\end{bmatrix}.\end{aligned} \tag{C1}$$

This gives immediately Eq. (4.10) if one inserts (C1) into Eq. (4.9) and selects due to the term $k_z\delta_{j3}$ of Eq. (3.20) the proper components. For the evaluation of Eq. (4.19) one needs

$$\langle BN(\alpha)\,|\,\hat{X}_j(\mathbf{k})\,|\,BN(\alpha;\beta\tilde{\beta})\rangle=\cos^2\alpha\left[g_{\pi NN}\sum_{st}^{1/2}d^{1/2}_{s\,1/2}(\beta)d^{1/2}_{t\,1/2}(\tilde{\beta})(\boldsymbol{\sigma}\cdot\mathbf{k})_{1/2s}(\tau_j)_{1/2t}\right]$$
$$+\cos\alpha\,\sin\alpha g_{\pi N\Delta}\left[\sum_{ST}^{3/2}d^{3/2}_{S\,1/2}(\beta)d^{3/2}_{T\,1/2}(\tilde{\beta})(\mathbf{S}^{\dagger}\cdot\mathbf{k})_{1/2S}(T_j^{\dagger})_{1/2T}\right]$$
$$+\sin\alpha\,\cos\alpha g_{\pi\Delta N}\left[\sum_{st}^{1/2}d^{1/2}_{s\,1/2}(\beta)d^{1/2}_{t\,1/2}(\tilde{\beta})(\mathbf{S}\cdot\mathbf{k})_{1/2s}(T_j)_{1/2t}\right]$$
$$+\sin^2\alpha g_{\pi\Delta\Delta}\left[\sum_{ST}^{3/2}d^{3/2}_{S\,1/2}(\beta)d^{3/2}_{T\,1/2}(\tilde{\beta})(\boldsymbol{\Sigma}\cdot\mathbf{k})_{1/2S}(\theta_j)_{1/2T}\right]. \tag{C2}$$

If one multiplies this with $\xi_j^*(\mathbf{k})$ or $\xi_j(\mathbf{k};\beta\tilde{\beta})$ one should keep in mind that afterwards one has to perform an integration over d^3k according to Eq. (4.19). However, both $\xi_j^*(\mathbf{k})$ and $\xi_j(k;\beta\tilde{\beta})$ are zero for $j=2$ and do not depend on k_y. Hence all terms of Eq. (C2) being proportional to k_y and δ_{j2} do not contribute to the integral and need not be evaluated. Using the matrices of Appendix A the rest can be written as

$$\langle BN(\alpha)\,|\,\hat{X}_j(\mathbf{k})\,|\,BN(\alpha;\beta\tilde{\beta})\rangle=g_{\pi NN}[A_{3z}(\alpha;\beta\tilde{\beta})\delta_{j3}k_z+A_{3x}(\alpha;\beta\tilde{\beta})\delta_{j3}k_x+A_{1z}(\alpha;\beta\tilde{\beta})\delta_{j1}k_z+A_{1x}(\alpha;\beta\tilde{\beta})\delta_{j1}k_x] \tag{C3}$$

with

$$A_{3z}(\alpha;\beta\tilde{\beta})=(\cos^2\alpha+\tfrac{4}{5}\sqrt{2}\sin\alpha\,\cos\alpha)d^{1/2}_{1/2\,1/2}(\beta)d^{1/2}_{1/2\,1/2}(\tilde{\beta})+(\tfrac{4}{5}\sqrt{2}\sin\alpha\,\cos\alpha+\tfrac{1}{5}\sin^2\alpha)d^{3/2}_{1/2\,1/2}(\beta)d^{3/2}_{1/2\,1/2}(\tilde{\beta})\ , \tag{C4a}$$

$$\begin{aligned}A_{3x}(\alpha;\beta\tilde{\beta})=&(\cos^2\alpha-\tfrac{2}{5}\sqrt{2}\sin\alpha\,\cos\alpha)d^{1/2}_{-1/2\,1/2}(\beta)d^{1/2}_{1/2\,1/2}(\tilde{\beta})\\&+(-\tfrac{2}{5}\sqrt{6}\cos\alpha\,\sin\alpha+\tfrac{1}{5}\sqrt{3}\sin^2\alpha)d^{3/2}_{3/2\,1/2}(\beta)d^{3/2}_{1/2\,1/2}(\tilde{\beta})\\&+(\tfrac{2}{5}\sqrt{2}\cos\alpha\,\sin\alpha+\tfrac{2}{5}\sin^2\alpha)d^{3/2}_{-1/2\,1/2}(\beta)d^{3/2}_{1/2\,1/2}(\tilde{\beta})\ ,\end{aligned} \tag{C4b}$$

$$\begin{aligned}A_{1z}(\alpha;\beta\tilde{\beta})=&(\cos^2\alpha-\tfrac{2}{5}\sqrt{2}\sin\alpha\,\cos\alpha)d^{1/2}_{1/2\,1/2}(\beta)d^{1/2}_{-1/2\,1/2}(\tilde{\beta})\\&+(-\tfrac{2}{5}\sqrt{6}\sin\alpha\,\cos\alpha+\tfrac{1}{5}\sqrt{3}\sin^2\alpha)d^{3/2}_{1/2\,1/2}(\beta)d^{3/2}_{3/2\,1/2}(\tilde{\beta})\\&+(\tfrac{2}{5}\sqrt{2}\sin\alpha\,\cos\alpha+\tfrac{2}{5}\sin^2\alpha)d^{3/2}_{1/2\,1/2}(\beta)d^{3/2}_{-1/2\,1/2}(\tilde{\beta})\ ,\end{aligned} \tag{C4c}$$

$$\begin{aligned}A_{1x}(\alpha;\beta\tilde{\beta})=&(\cos^2\alpha+\tfrac{1}{5}\sqrt{2}\sin^2\alpha)d^{1/2}_{-1/2\,1/2}(\beta)d^{1/2}_{-1/2\,1/2}(\tilde{\beta})+(-\tfrac{1}{5}\sqrt{6}\sin\alpha\,\cos\alpha+\tfrac{2}{5}\sqrt{3}\sin^2\alpha)d^{3/2}_{3/2\,1/2}(\beta)d^{3/2}_{-1/2\,1/2}(\tilde{\beta})\\&+(\tfrac{1}{5}\sqrt{2}\sin\alpha\,\cos\alpha+\tfrac{4}{5}\sin^2\alpha)d^{3/2}_{-1/2\,1/2}(\beta)d^{3/2}_{-1/2\,1/2}(\tilde{\beta})\\&+(-\tfrac{1}{5}\sqrt{6}\sin\alpha\,\cos\alpha+\tfrac{2}{5}\sqrt{3}\sin^2\alpha)d^{3/2}_{-1/2\,1/2}(\beta)d^{3/2}_{3/2\,1/2}(\tilde{\beta})\\&+(\tfrac{3}{5}\sqrt{2}\sin\alpha\,\cos\alpha+\tfrac{3}{5}\sin^2\alpha)d^{3/2}_{3/2\,1/2}(\beta)d^{3/2}_{3/2\,1/2}(\tilde{\beta})\ .\end{aligned} \tag{C4d}$$

Inserting Eqs. (C3) and (C4) into Eq. (4.19) yields

$$\begin{aligned}h_{\rm coupl}(\alpha,R;\beta\tilde{\beta})=n_\pi(\alpha;\beta\tilde{\beta})\int d^3k\frac{f_R{}^2(k)}{\omega(k)}\\&\times[A_{3z}(\alpha;\beta\tilde{\beta})k_z{}^2\cos\beta\cos\tilde{\beta}-A_{3x}(\alpha,\beta\tilde{\beta})k_x{}^2\sin\beta\cos\tilde{\beta}\\&-A_{1z}(\alpha;\beta\tilde{\beta})k_z{}^2\cos\beta\sin\tilde{\beta}+A_{1x}(\alpha;\beta\tilde{\beta})k_x{}^2\sin\beta\sin\tilde{\beta}+A_{3z}(\alpha;\beta\tilde{\beta})k_z{}^2]\ .\end{aligned} \tag{C5}$$

The integration over k with Eq. (B4) yields then Eq. (4.20).

APPENDIX D: VERTEX RENORMALIZATION DUE TO PROJECTION

The final expression for $p(\alpha)$ is

$$\begin{aligned}p(\alpha)=\frac{1}{9N_J}\int_0^\pi d\beta\sin\beta\int_0^\pi d\tilde{\beta}\sin\tilde{\beta}n_\pi(\alpha;\beta\tilde{\beta})\\&\times\{(\cos^2\alpha+\tfrac{4}{5}\sqrt{2}\cos\alpha\,\sin\alpha)[d^{1/2}_{1/2\,1/2}(\beta)]^2[d^{1/2}_{1/2\,1/2}(\tilde{\beta})]^2\\&+(2\cos^2\alpha-\tfrac{4}{5}\sqrt{2}\cos\alpha\,\sin\alpha)[d^{1/2}_{-1/2\,1/2}(\beta)]^2[d^{1/2}_{1/2\,1/2}(\tilde{\beta})]^2\end{aligned}$$

$$+(2\cos^2\alpha-\tfrac{4}{5}\sqrt{2}\cos\alpha\sin\alpha)[d^{1/2}_{1/2\,1/2}(\beta)]^2[d^{1/2}_{-1/2\,1/2}(\tilde{\beta})]^2$$

$$+(4\cos^2\alpha+\tfrac{4}{5}\sqrt{2}\cos\alpha\sin\alpha)[d^{1/2}_{-1/2\,1/2}(\beta)]^2[d^{1/2}_{-1/2\,1/2}(\tilde{\beta})]^2$$

$$+(\tfrac{4}{5}\sqrt{2}\cos\alpha\sin\alpha+\tfrac{1}{5}\sin^2\alpha)[d^{1/2}_{1/2\,1/2}(\beta)d^{3/2}_{1/2\,1/2}(\beta)][d^{1/2}_{1/2\,1/2}(\tilde{\beta})d^{3/2}_{1/2\,1/2}(\tilde{\beta})]$$

$$+(\tfrac{4}{5}\sqrt{2}\cos\alpha\sin\alpha+\tfrac{4}{5}\sin^2\alpha)[d^{1/2}_{-1/2\,1/2}(\beta)d^{3/2}_{-1/2\,1/2}(\beta)][d^{1/2}_{1/2\,1/2}(\tilde{\beta})d^{3/2}_{1/2\,1/2}(\tilde{\beta})]$$

$$+(\tfrac{4}{5}\sqrt{2}\cos\alpha\sin\alpha+\tfrac{4}{5}\sin^2\alpha)[d^{1/2}_{1/2\,1/2}(\beta)d^{3/2}_{1/2\,1/2}(\beta)][d^{1/2}_{1/2\,1/2}(\tilde{\beta})d^{3/2}_{-1/2\,1/2}(\tilde{\beta})]$$

$$+(\tfrac{4}{5}\sqrt{2}\cos\alpha\sin\alpha+\tfrac{16}{5}\sin^2\alpha)[d^{1/2}_{-1/2\,1/2}(\beta)d^{3/2}_{-1/2\,1/2}(\beta)][d^{1/2}_{-1/2\,1/2}(\tilde{\beta})d^{3/2}_{-1/2\,1/2}(\tilde{\beta})]\}\ .$$

---

*On leave from Departamento de Fisica, Universidade de Coimbra, P-3000 Coimbra, Portugal.

†Also at Institut für Theoretische Kernphysik, Universität Bonn, D-5300 Bonn, West Germany.

[1]R. Goldflam and L. Wilets, Phys. Rev. D **25**, 1951 (1982); Th. Köppel and M. Harvey, *ibid.* **31**, 171 (1985).

[2]G. Adkins, C. Nappi, and E. Witten, Nucl. Phys. **B228**, 552 (1983).

[3]M. C. Birse and M. K. Banerjee, Phys. Lett. **136B**, 284 (1984).

[4]G. Kälbermann and J. M. Eisenberg, Phys. Lett. **139B**, 337 (1984).

[5]G. E. Brown, A. D. Jackson, M. Rho, and V. Vento, Phys. Lett. **140B**, 285 (1984).

[6]S. Kahana, G. Ripka, and V. Soni, Nucl. Phys. **A415**, 351 (1984).

[7]A. Chodos and C. B. Thorn, Phys. Rev. D **12**, 2733 (1975).

[8]G. E. Brown and M. Rho, Phys. Lett. **82B**, 177 (1979).

[9]G. E. Brown, M. Rho, and V. Vento, Phys. Lett. **84B**, 383 (1979).

[10]V. Vento, M. Rho, E. M. Nyman, J. H. Inn, and G. E. Brown, Nucl. Phys. **A345**, 413 (1980).

[11]G. A. Miller, A. W. Thomas, and S. Théberge, Phys. Lett. **91B**, 192 (1980).

[12]S. Théberge, A. W. Thomas, and G. A. Miller, Phys. Rev. D **22**, 2838 (1980).

[13]A. W. Thomas, Adv. Nucl. Phys. **13**, 1 (1983).

[14]G. E. Brown, Nucl. Phys. **A358**, 39c (1981).

[15]J. de Kam and H. J. Pirner, Nucl. Phys. **A389**, 640 (1982).

[16]J. N. Urbano and K. Goeke, Phys. Lett. **143B**, 319 (1984).

[17]A. Chodos, R. L. Jaffe, K. Johnson, C. B. Thorn, and V. F. Weisskopf, Phys. Rev. D **9**, 3471 (1974); A. Chodos, R. L. Jaffe, K. Johnson, and C. B. Thorn, *ibid.* **10**, 2599 (1974).

[18]C. E. DeTar, Phys. Rev. D **24**, 752 (1981); **24**, 762 (1981).

[19]V. Vento, Phys. Lett. **107B**, 5 (1981).

[20]J. Urbano, M. Fiolhais, and J. Pacheco, in *Quarks, Mesons and Isobars in Nuclei,* proceedings of the 5th Topical School, Motril, Granada, Spain, 1982, edited by R. Guardiola and A. Polls (World Scientific, Singapore, 1982), p. 314.

[21]W. Weise, in *Quarks, Mesons and Isobars in Nuclei* (Ref. 20), p. 146.

[22]S. J. Brodsky and G. P. Lepage, Phys. Scr. **23**, 945 (1981).

[23]J. da Providencia, Nucl. Phys. **B57**, 536 (1973).

[24]J. da Providencia and J. N. Urbano, Phys. Rev. D **18**, 4208 (1978).

[25]E. M. Henley and W. Thirring, *Elementary Quantum Field Theory* (McGraw-Hill, New York, 1962), Chap. 18.

[26]K. Goeke, A. Faessler, and H. H. Wolter, Nucl. Phys. **A183**, 352 (1972).

[27]G. E. Brown and W. Weise, Phys. Rep. **22C**, 280 (1975).

[28]C. E. Carlson, T. H. Hansson, and C. Peterson, Phys. Rev. D **27**, 1556 (1983).

[29]T. DeGrand, R. L. Jaffe, K. Johnson, and J. Kiskis, Phys. Rev. D **12**, 2060 (1975).

[30]M. Fiolhais, J. N. Urbano, and K. Goeke, Phys. Lett. **150B**, 253 (1985).

[31]G. E. Brown and M. Rho, Phys. Today **36** (No. 2), 24 (1983).